DANMARKS OG GRØNLANDS GEOLOGISKE UNDERSØGELSE RAPPORT 1998/12

A scanning electron microscopy study of ash, char, deposits and fuels from straw combustion and co-combustion of coal and straw

Henning Sund Sørensen

GEOLOGICAL SURVEY OF DENMARK AND GREENLAND
MINISTRY OF ENVIRONMENT AND ENERGY

G E U S

DANMARKS OG GRØNLANDS GEOLOGISKE UNDERSØGELSE RAPPORT 1998/12

A scanning electron microscopy study of ash, char, deposits and fuels from straw combustion and co-combustion of coal and straw

Henning Sund Sørensen

GEOLOGICAL SURVEY OF DENMARK AND GREENLAND
MINISTRY OF ENVIRONMENT AND ENERGY

GEUS

Index

1. Introduction

As a measure to meet the demand for reduction of CO_2 emissions the Danish Government has commited the Danish Power Companies to burn between 1 and 1.2 million tons of straw per year by the year 2000. Therefore a considerable research effort is put into solving problems that may arise by shifting from the presently dominating coal fuel to biomass. Biomass in general has a quite different chemical composition than coal with respect to the contents of both organic and inorganic constituents as well as heating value.

The main surplus of biomass in Denmark is straw and therefore the efforts are concentrated on this biomass fuel. One of the main problems involved in straw combustion is related to the behaviour and fate of the ash forming inorganic species in the fuel. These elements can end up in fly ash, bottom ash or may be incorporated in various types of deposits on boiler surfaces. The presence of deposits can reduce the heat transfer and increase the temperature level in the boiler. Other significant problems involve corrosion beneath deposits and large blocks falling down due to gravity forces thereby damaging the boiler.

Clearly the fate of the inorganic constituents during combustion and deposition depends on their mode of occurrence in the straw. The inorganic species in straw can occur either disseminated or ionically bound in the organic structure, be located in inorganic straw constituents or can be constituents of incorporated terrigeneuos soil particles. Additional factors, such as combustion temperature and boiler design, also influence the fate of inorganic material during combustion.

Knowledge of straw ash composition and melting behaviour is important to be able to foresee, at least to some extent, the fate of the inorganic elements in terms of practical operation of boilers. The aim is to be able to predict and possibly avoid formation of troublesome deposits and potential corrosion. Additionally, knowledge of straw ash compositions and morphology is useful for possible utilization or disposal of the ash. An extensive Scanning Electron Microscopy (SEM) study of straw ash has been

performed at the Geological Survey of Denmark and Greenland (GEUS) as part of the EFP-95 project on *Characterization of Biomass Ashes* (Frandsen et al., 1998a). In addition the study encompassed wheat straw and wheat grains as representatives of different fuels as well as various deposits to study how ash can contribute to deposit formation. The study at GEUS was performed on a Philips XL40 SEM equipped with a Voyager 2.7 EDX analysis software package. The main incentive was to develop a technique for straw ash characterization by Computer Controlled Scanning Electron Microscopy (CCSEM) based on a well-established technique for minerals in coal (Laursen, 1997a).

This report firstly presents representative SEM images that were obtained during the study for future reference. Secondly a presentation and discussion of CCSEM results is provided.

2. Sample material

The samples that are presented in this report were obtained from different sources. Bottom ash and fly ash were obtained from the straw-fired Haslev and Slagelse Combined Heat and Power plants (CHP). Deposits from straw combustion were obtained from two experiments: Slagelse 3 and Haslev 1, burning barley and wheat, respectively.

Full scale co-combustion samples were obtained from the pulverized fuel (pf) - fired MKS1 boiler at Studstrupværket. Fuel (coal and wheat straw), char, bottom ash and fly ash were analyzed by CCSEM and deposits by Scanning Electron Microscopy Point Counting (SEMPC).

Laboratory ashes were produced at dK-Teknik from wheat straw and wheat grains. Additionally, a series of laboratory ashes were produced from fuels used at MKS1 at Studstrupværket, namely a Columbian bituminous coal and danish wheat straw. Mixed ashes were produced both by mixing the fuels before ashing and by ashing the fuels separately followed by physical mixing.

3. SEM images

This section contains the SEM images that were obtained during the project. Most of the images were obtained to give representative images of the various samples: wheat straw, wheat grain, straw chars, bottom ash, fly ash, laboratory ash and deposits. Brief descriptions of the samples and the observed features can be found in the figure captions. The descriptions are not meant to be complete and emphasis has been put on the inorganic components. The majority of the images were obtained on embedded polished samples with the Backscattered Electron Detector (BSE). In BSE images brightness is proportional to average atomic number, i.e. most inorganic particles will show up bright compared to organic substances such as carbonaceous matter and embedding material.

Approximately 0.2-2 grams of material were used depending on the available amount. The samples were blended with Epofix or Carnauba Wax during thorough mixing and was left to harden. In the case of Epofix the hardened block were sectioned perpendicular to the direction of sedimentation and subsequently embedded with the new face pointing upwards. By analyzing the whole cross section any bias due to gravity fractionation is avoided. In the case of Carnauba Wax no perpendicular sectioning was performed since the wax hardens almost immediately leaving no time for sedimentation. The blocks were ground and polished with the last step being 0.25 micron diamond paste and subsequently coated with a thin carbon layer in a Polaron TB500 Coater. During handling of the samples no water or alcohol were utilized, since these compounds may cause dissolution of salts. For lubrication and cooling during grinding and polishing either Buehler lapping oil or distilled petroleum were used. Images of straw chars were obtained on powder samples, i.e. samples that were distributed loosely on carbon tape mounted on a sample holder and subsequently coated with carbon.

3.1 Danish wheat straw and wheat grain.

The samples were studied to evaluate mineral compositions and to assess the extent to which CCSEM analyses is suited to characterize and quantify inorganic constituents of biomass fuels.

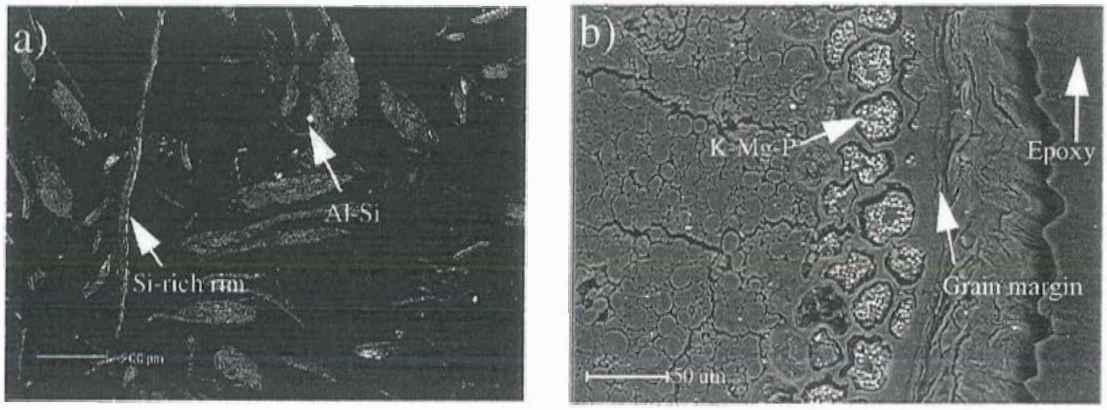

Fig.3.1. Representative images of biomass fuel examples.

a) Milled wheat straw. The inorganic or inorganic-rich constituents show up bright compared to the organic material. Most conspicuous is an elongated rim covering the length of one thin straw fragment. This type of rim is a common feature in the straw and is mainly composed of Si (>90%). Additional inorganic particles consist mainly of terrigeneous derived clay (Al-Si) or quartz particles.

b) Wheat grain margin. The major part of the inorganic-rich particles are located close to the wheat grain boundary as small K, Mg and P rich spherical particles arranged in clusters. These are phytates which function as important storage-location of the nutrients K and P (Marschner, 1995).

There is an obvious difference in the composition of inorganic particles in the straw and in the grain, the straw being dominated by silica whereas the grain is dominated by K and P rich particles. However, inorganic elements that are disseminated or bound in the organic structure is not readily discernible in the BSE image. This means that, because CCSEM analysis is controlled by contrasts in BSE images, elements that largely are organically associated in low concentrations, as for example K and Ca, are not detected (section 4.1).

3.2 Bottom ash and fly ash from straw fired plants: Haslev CHP and Slagelse CHP

Bottom ash and fly ash were sampled at two danish straw fired boilers in due of an earlier biomass characterization project (Stenholm et al., 1996). Fly ash was collected in a bag-filter at Haslev CHP and in an electro-filter at Slagelse CHP. Bottom ash was collected from material that was automatically scraped off the bottom grate in both cases. Four of the experiments utilized wheat straw, one used barley straw and one rape straw (Table 3.1). All ash samples were subjected to CCSEM analysis (Sørensen, 1997), and the complete CCSEM results can be found in Frandsen et al. (1998b). In this section representative BSE images of the analyzed samples are presented.

Table 3.1

Experiment	Fuel
Haslev 1	Wheat
Slagelse 1	Wheat
Slagelse 3	Barley
Slagelse 6	Wheat
Slagelse 7	Wheat
Slagelse 8	Rape

3.2.1. Bottom ash

The bottom ash samples were milled at dK-Teknik to be used for traditional fusion measurements. Therefore the form and size of the particles is not neccesarily representative of original features.

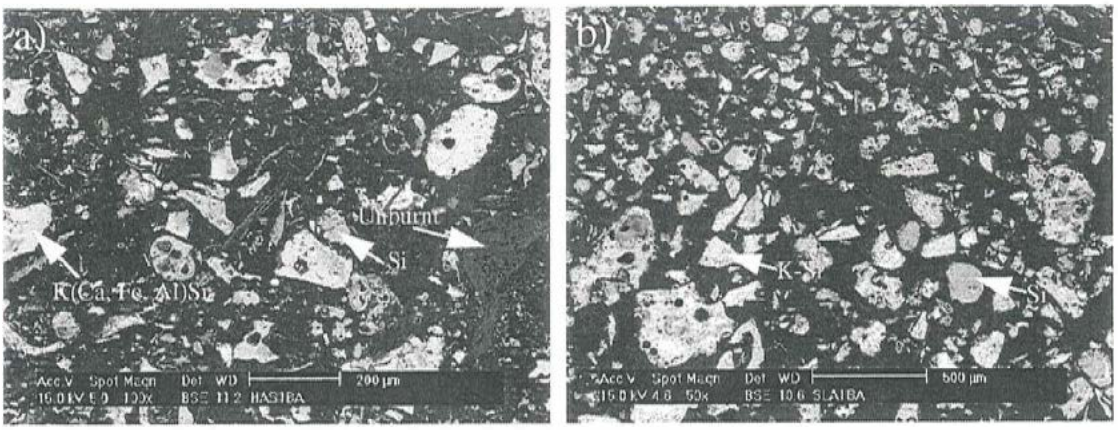

Fig.3.2a-b. Representative BSE-images of bottom ash from Slagelse and Haslev CHP (see figure captions om following page).

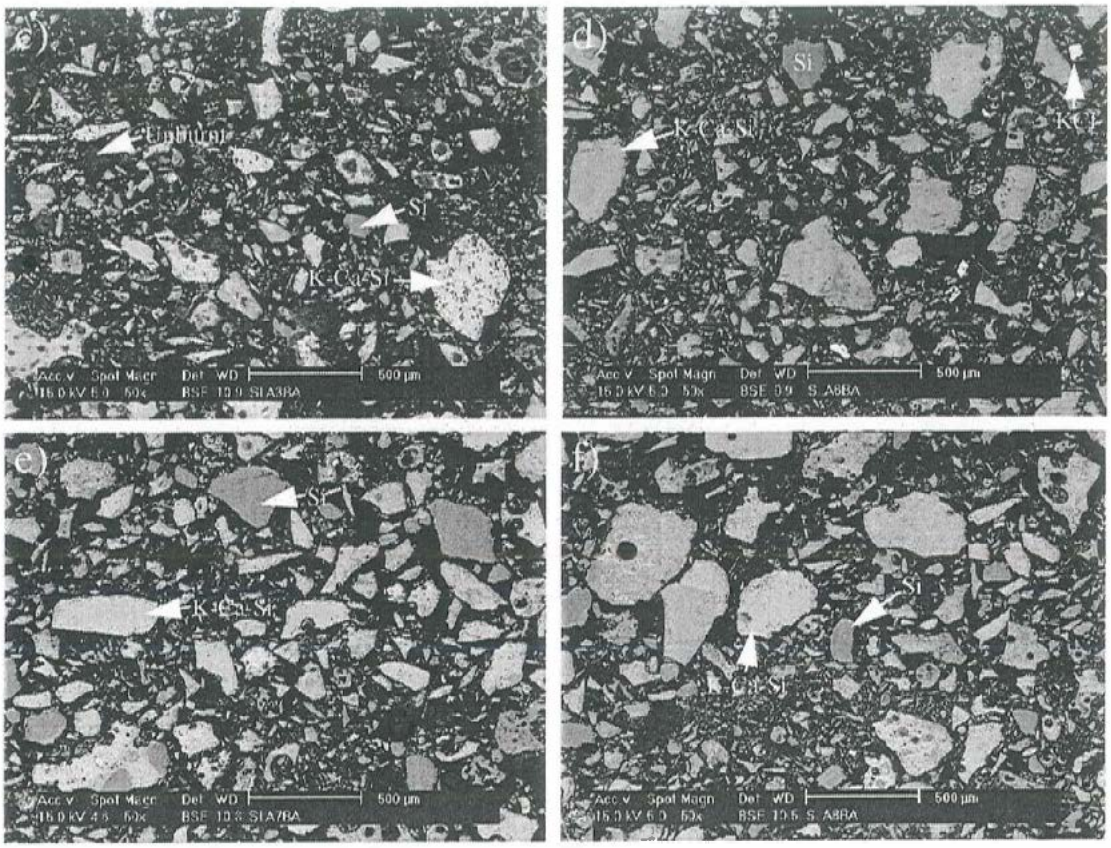

Fig.3.2c-f. Representative BSE-images of bottom ash from Slagelse and Haslev CHP.

a) Bottom ash from Haslev 1 (HASIBA). Ash particles range in size from around 1 micron up to 200 micron. Variable BSE reflection in individual particles evidence that the particles are composite. Commonly they are composed of a Si-rich area or core (medium grey) associated with a (probably) fused mass of K-(Ca-Fe-Al) rich silica material (white or light grey). An example of this type of zoning is illustrated in Fig.3.3. Straw char particles(dark grey) are also present.

b) Bottom ash from Slagelse 1 (SLA1BA). Particle compositions are similar to the ones observed in a). The vertical variation in particle size is an effect of sedimentation during sample preparation. In CCSEM analysis this fractionation is taken into account by analyzing a whole cross section.

c) Bottom ash from Slagelse 3 (SLA3BA). The image is dominated by K-Ca-Si rich and Si-rich particles.

d) Bottom ash from Slagelse 6 (SLA6BA). In addition to silica-rich particles several crystals of KCl up to 20 micron are observed.

e) Bottom ash from Slagelse 7 (SLA7BA). The image is dominated by silica rich composite particles ranging in size up to around 300 micron.

f) Bottom ash from Slagelse 8 (SLA8BA). The image is dominated by silica rich composite particles ranging in size from 1 micron up to 500 micron.

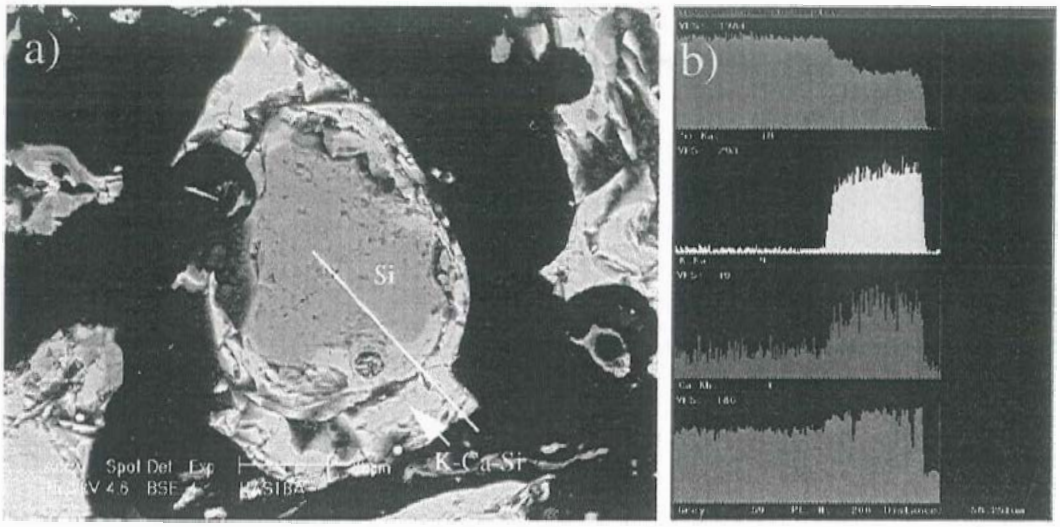

Fig.3.3. Compositional zoning in bottom ash particle from Haslev 1 (HAS1BA).

a) Shows the outline of a 100 micron silica-rich bottom ash particle. The white line shows the location of line scan, b) line scan illustrating relative distribution of, from the top down, Si, K, Ca and BSE grey level. The K and Ca content increases whereas the Si content decreases gradually outwards over a distance of ca. 10 micron. The line scan is 58.25 microns long.

3.2.2. Fly ash

During preparation of the fly ash samples they were thorougly mixed with epoxy to separate lumps of material that may have formed during sampling or in the sample container. However, as illustrated below much of the fine grained material appears in aggregates in several of the samples (Fig.3.4).

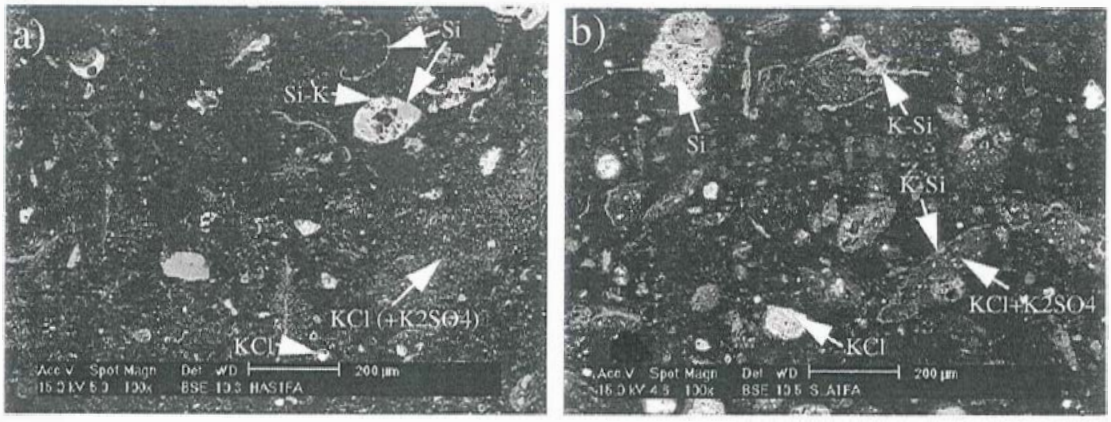

Fig.3.4a-b. Representative BSE-images of fly ash samples from Haslev and Slagelse CHP (see figure captions on following page).

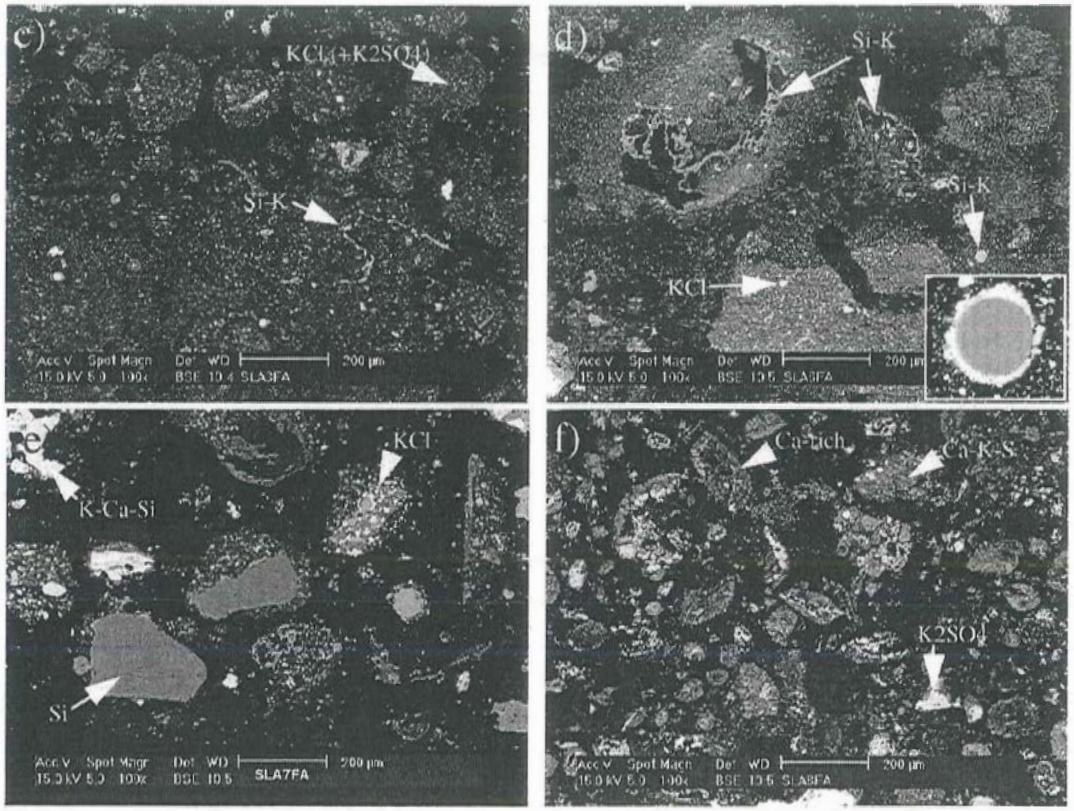

Fig.3.4c-f. Representative BSE-images of fly ash samples from Haslev and Slagelse CHP.

a) Fly ash from Haslev 1(HAS1FA). The fly ash contains much fine grained (submicron to micron) material and several larger (circa 20-150 micron) particles. Individual submicron particles are too small to analyze, but qualitative SEM/EDX show that they mainly consist of KCl with subordinate K_2SO_4 and small silica-rich particles. In CCSEM analyses these masses of fine-grained material are commonly analyzed as one big particle because they can not be separated on the basis of a backscatter image. Thin elongated Si-K rich rims up to 200 micron long are typically associated with aggregates of fine material. Composite silica-rich particles similar to the ones observed in the bottom ashes are also present.

b) Fly ash from Slagelse 1 (SLA1FA). This sample is similar to the Haslev 1 fly ash. Much of the submicron material masses is associated with Si-K rich rims.

c) Fly ash from Slagelse 3 (SLA3FA). In this sample almost all of the submicron material occurs in rounded aggregates up to 200 micron across. Si-K rich rims are associated with such masses.

d) Fly ash from Slagelse 6 (SLA6FA). This image shows quite large (up to 0.5 mm) masses of submicron particles. Bright appearing KCl crystals appear to be larger in this sample than in the other fly ashes. The lower right insert shows a spherical Si-K rich particle with a rim of KCl.

e) Fly ash from Slagelse 7 (SLA7FA). Contains relatively large (50-200 micron) Si-rich particles with attached masses of KCl and minor K_2SO_4. Also present are large particles consisting of K, Ca and Si.

f) Fly ash from Slagelse 8 (SLA8FA). This sample is different from the remaining fly ash samples, reflecting that it originated from rape combustion. Rape has a contrasting composition compared to wheat and barley especially in terms of higher Ca and S and lower Si-content. Most of the particles or masses of particles are rich in Ca, and are probably mixtures of $CaSO_4$, Ca-oxide and K_2SO_4.

3.2.3. Comments to observations of bottom ash and fly ash from Haslev CHP and Slagelse CHP

Generally bottom ashes are dominated by relatively large silica-rich particles, most of them containing K and subordinate Ca. Many of the particles are composite with domains of almost pure Si. It appears that the Si in the straw have reacted to varying degrees with loosely bound metals, especially K that were evaporated during combustion. The extent to which this process have occurred indicates that the process took place over some time, i.e. until the bottom ash were scraped off the grate. A line scan extending from a Si-rich core to the surrounding K and Ca enriched margin illustrated that the change in composition occurs gradually over a distance of approximately 10 microns (Fig.3.3). The shape and size of the gradient makes is likely that the reaction between K and the Si-particle is diffusion controlled. In summary it appears that K is bound to a significant extent to silica in the bottom ash.

The fly ash is dominated by submicron or micron-sized particles of primarily KCl with subordinate K_2SO_4 and silica-rich compounds (Fig.3.4). These particles are commonly present in clusters or aggregates that can reach a size of up to 0.5 mm. These large masses probably formed during fly ash sampling or handling. However, minor attachment of fly ash particles to each other or to larger silica-rich particles is common and is believed to have formed in the boiler. The fly ash formed in rape combustion (SLA8FA) is clearly different from fly ash from wheat and barley combustion, especially in terms of a higher content of Ca and S rich particles. However, the bottom ash formed during rape combustion (SLA8BA) does not distinguish itself significantly, probably as a result of carry over of material from the former experiment that utilized wheat as fuel.

3.3 Deposits from the Haslev 1 and the Slagelse 3 experiments.

Deposits were collected in the Haslev and Slagelse CHP's on water-cooled deposition probes. Probes were placed both in the furnace and in the superheater region (Fig.3.5). After sampling the deposits were first brushed off with a soft brush ("outer" loose part of deposit), and afterwards with a hard brush ("inner" hard part of deposit). The deposit samples were embedded, polished and subjected to CCSEM analysis (section 4.3.2). Representative BSE images of the polished, embedded samples are shown in Figure 3.6.

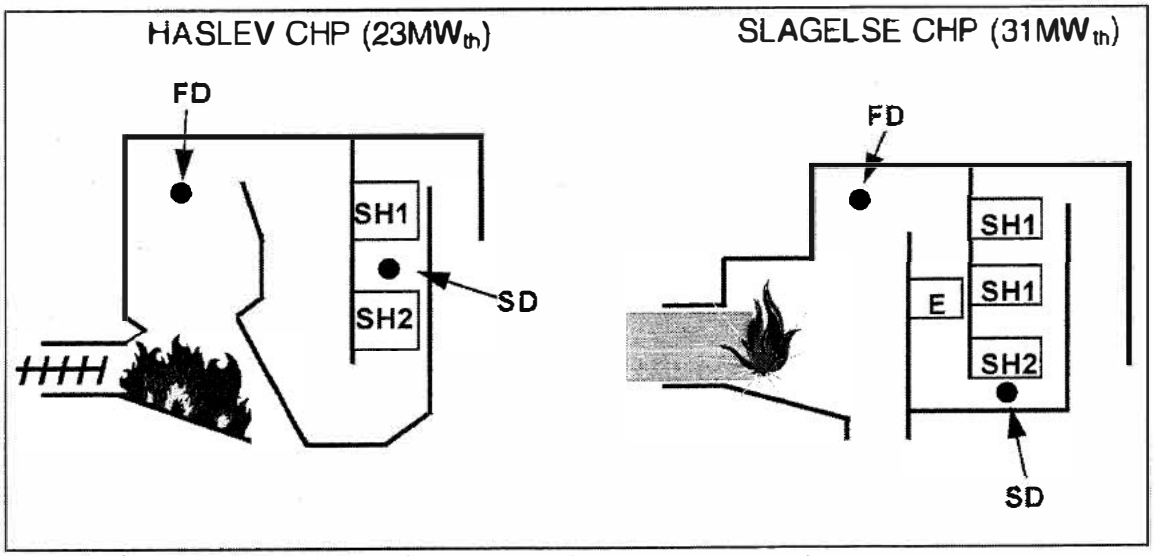

Fig. 3.5. Schematic illustrations of boiler designs for Haslev CHP and Slagelse CHP. Arrows indicate location of deposit probes in the furnace (FD) and in the superheater region (SD) (modified after Hansen et al., 1997)

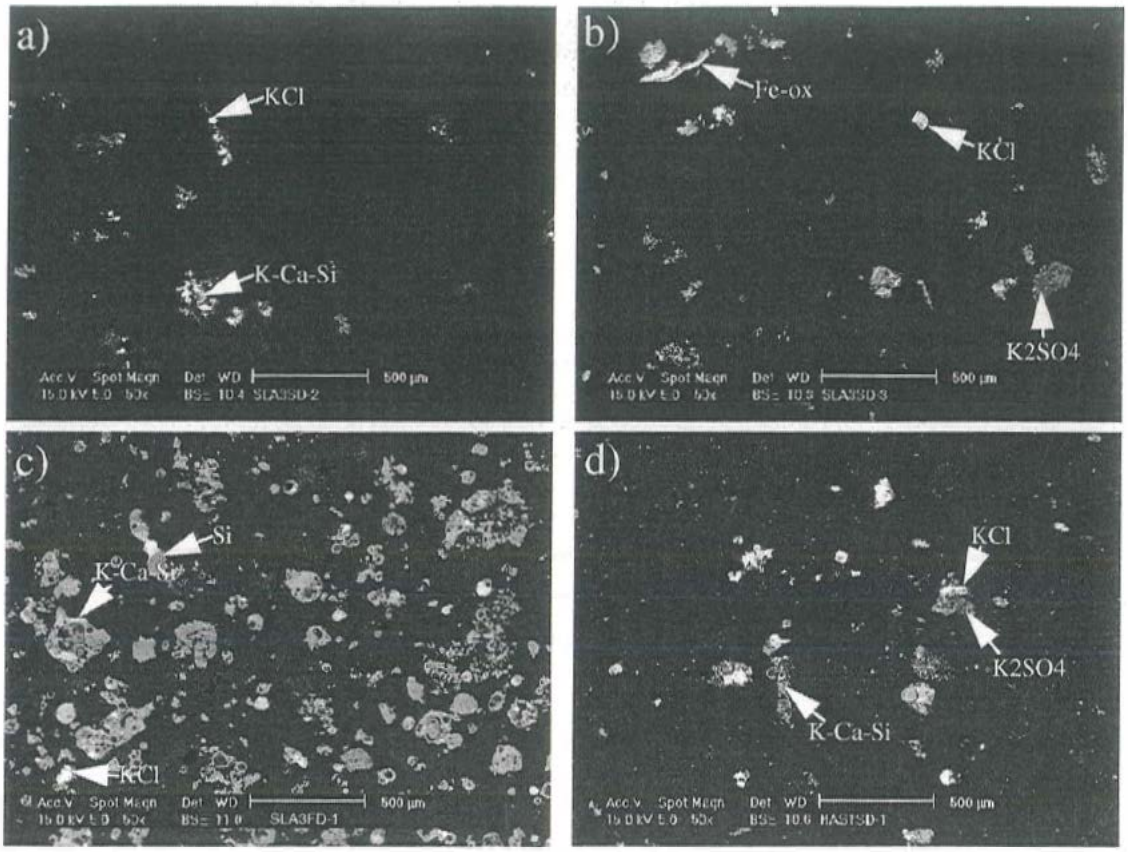

Fig.3.6a-d. Representative BSE-images of deposits from Haslev and Slagelse CHP

a) SLA3SD-2 (outer superheater deposit). The sample consists mainly of small (< 50 micron) KCl particles and subordinate probably amorphous K-Ca silicates (particles rich in K, Ca and Si).

b) SLA3SD-3 (inner superheater deposit). The sample consists primarily of KCl with subordinate K_2SO_4. Some Fe-oxide is present as well, probably being disrupted scales of the oxidized probe metal surface.

c) SLA3FD-1 (outer furnace deposit). The deposit is dominated by silica-rich particles from 5 to 150 micron. Some KCl is also present mostly being attached to silica particles. The silica-rich particles contain varying amounts of K and Ca.

d) HASISD-1 (superheater deposit). The image shows KCl crystals associated with K_2SO_4 and K-Ca silicate.

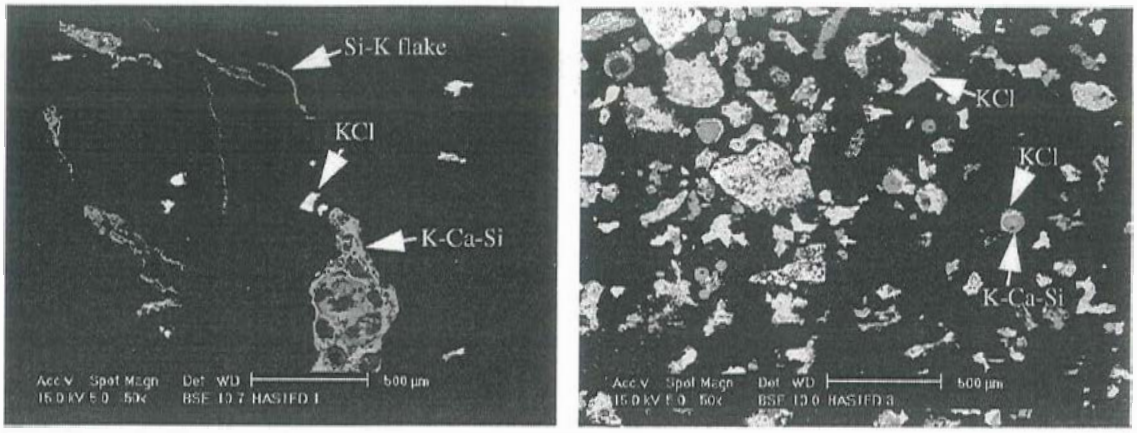

Fig.3.6e-f. Representative BSE-images of deposits from Slagelse CHP

e) HASIFD-1 (outer furnace deposit). The image shows the presence of KCl and large fused amorphous K-Ca silicate. Thin K-Ca-Si rich flakes are also present.

f) HASIFD-3 (inner furnace deposit). The image shows a predominance of KCl and subordinate K-Ca silicates that are often spherical and with attached KCl rims.

3.3.1. Comments to observations on deposits from Haslev 1 and Slagelse 3

Generally the furnace deposits are primarily composed of KCl, K-Ca silicates and K_2SO_4. The silicates commonly appear fused either in the form of amorphous particles or as minor spherical fly ash particles. KCl occur either as submicron to micron sized particles commonly together with K_2SO_4 as singular larger particles or as coatings on silicates.

3.4 Fuels from co-combustion at MKS1, Studstrupværket

Fuels from the experiments 3, 4 and 5 at MKS1 at Studstrupværket were analyzed by CCSEM (Appendix G in Frandsen et al., 1998a). The coal utilized in all three cases were a Columbian high volatile bituminous coal whereas the feedstock straw was wheat. Representative images of the fuels are shown in Fig.3.7.

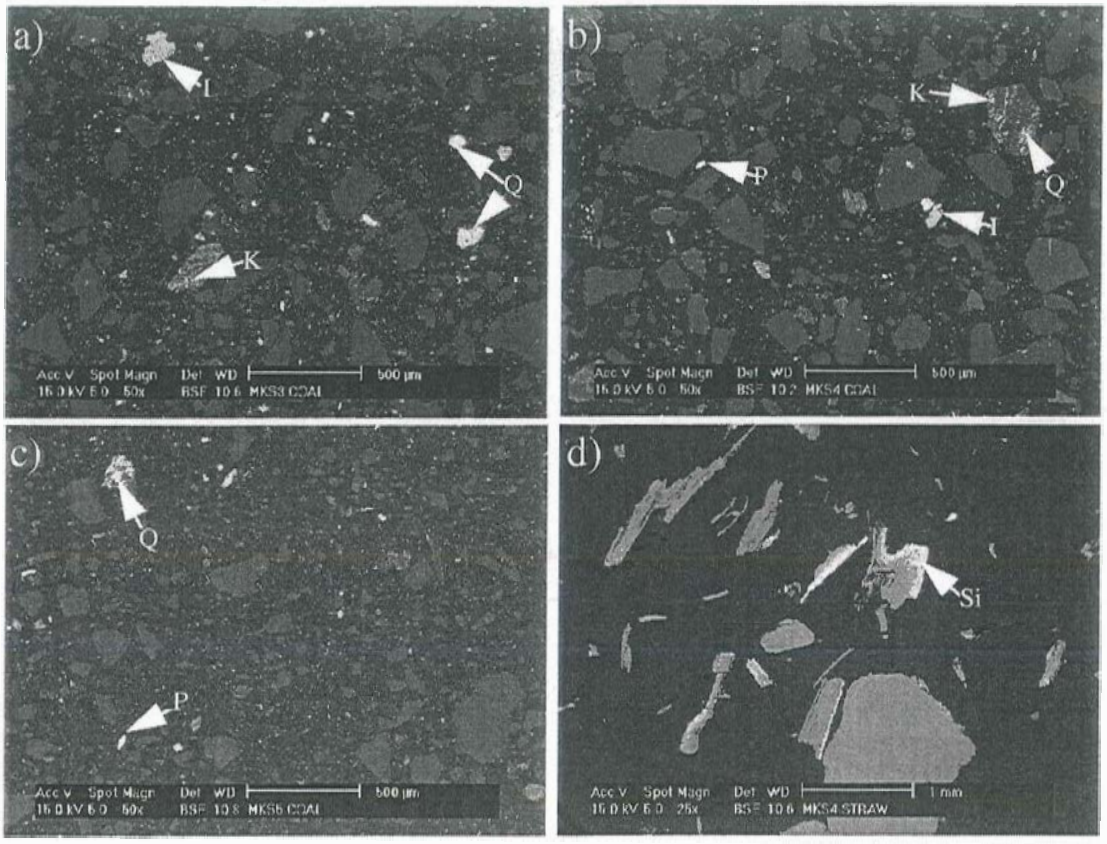

Fig.3.7. Representative images of fuels from MKS1.

a-c) The BSE images show coals from experiments 3, 4 and 5 (MKS3C, MKS4C and MKS5C). The coal particles appear light grey whereas the associated minerals appear bright. The mineral association is dominated by quartz (Q), various clay minerals (K: kaolinite and I: illite) as well as minor pyrite (P).

d) Straw utilized in experiment 4 (MKS4S) as an example of the wheat straw used at MKS1. The straw was milled before sampling rendering fragments up to around 2 mm in size. The image shows the common presence of Si-rich margins partially outlining straw fragments.

3.5 Straw chars sampled from the burner zone at MKS1

Combustion chars were sampled from the burner zone at MKS1 during three experiments with addition of 20% (exp.2), 10% (exp.4) and 0% straw (exp.9), respectively. Sampling was performed with a suction pyrometer that extended into a part of the burner zone where mixing of coal and straw occured (Fig.3.10). Therefore both straw chars and coal chars were sampled. The chars were collected on a sintered copper filter with a nominal pore size of 40 micron. However, the filter-pores were progressively blocked during the sampling time of approximately 30 seconds meaning that smaller particles may have been retained during the last phases of sampling. The

char samples illustrated in Figs. 3.8 and Fig 3.9 were subjected to CCSEM analysis (section 4.4).

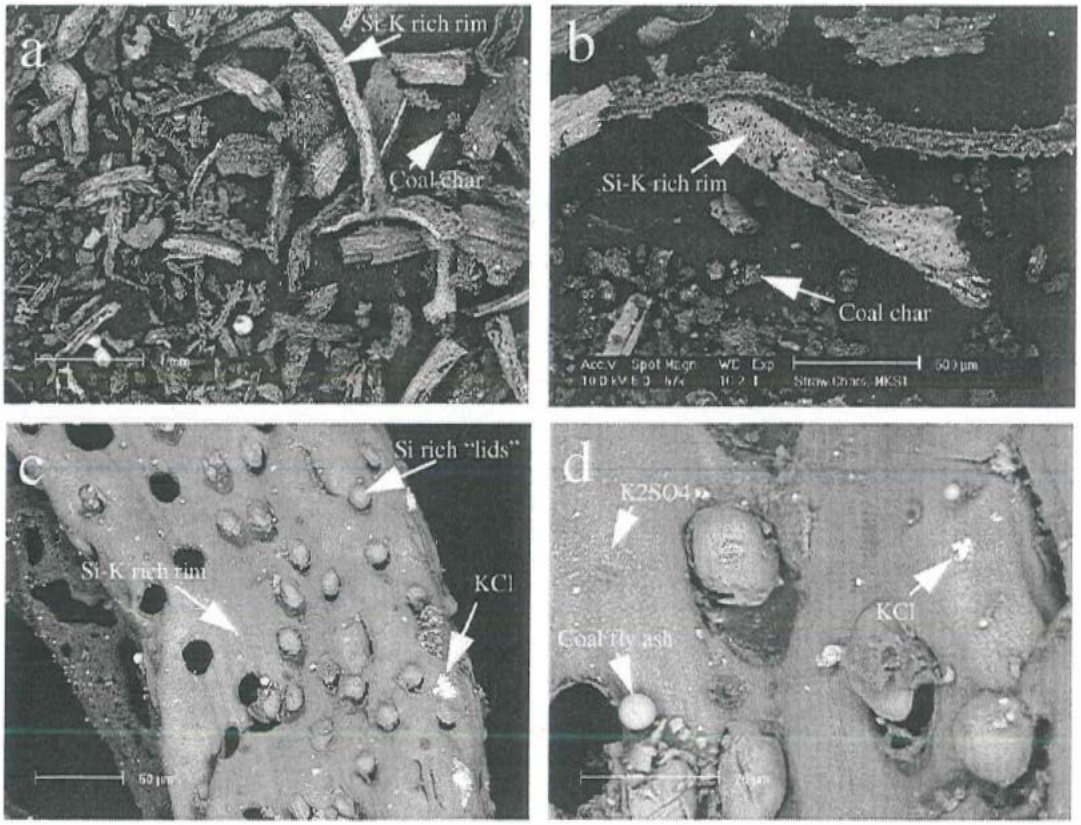

Fig.3.8a-d. Representative BSE images of char powder samples (experiment 2, 20% straw, 75% load).

a) The straw chars are typically elongated and up to 2 mm long, retaining parts of the straw structure. Conspicuous Si-K rich rims are commonly present on the surface of the chars. Coal chars are typically much smaller (around 100 microns) and rounded.

b) The image illustrates the distinct difference between the straw chars with partially broken Si-K rich rims and the rounded coal chars.

c) Shows detail of Si-K rich rim on straw char. The rim contains a multitude of approximately 15 micron large round or oval Si-rich "lids". The origin of this structure is unknown, but it is speculated that it is determined by the original structure of the straw. Also seen are bright appearing KCl crystals attached to the rim.

d) Shows detail of Si-K rich rim. The Si-rich lids are partially detached. Also seen are KCl crystals and a spherical coal-derived alumino-silicate fly ash particle. On the Si-K rich rim a thin coating of K_2SO_4 is observed.

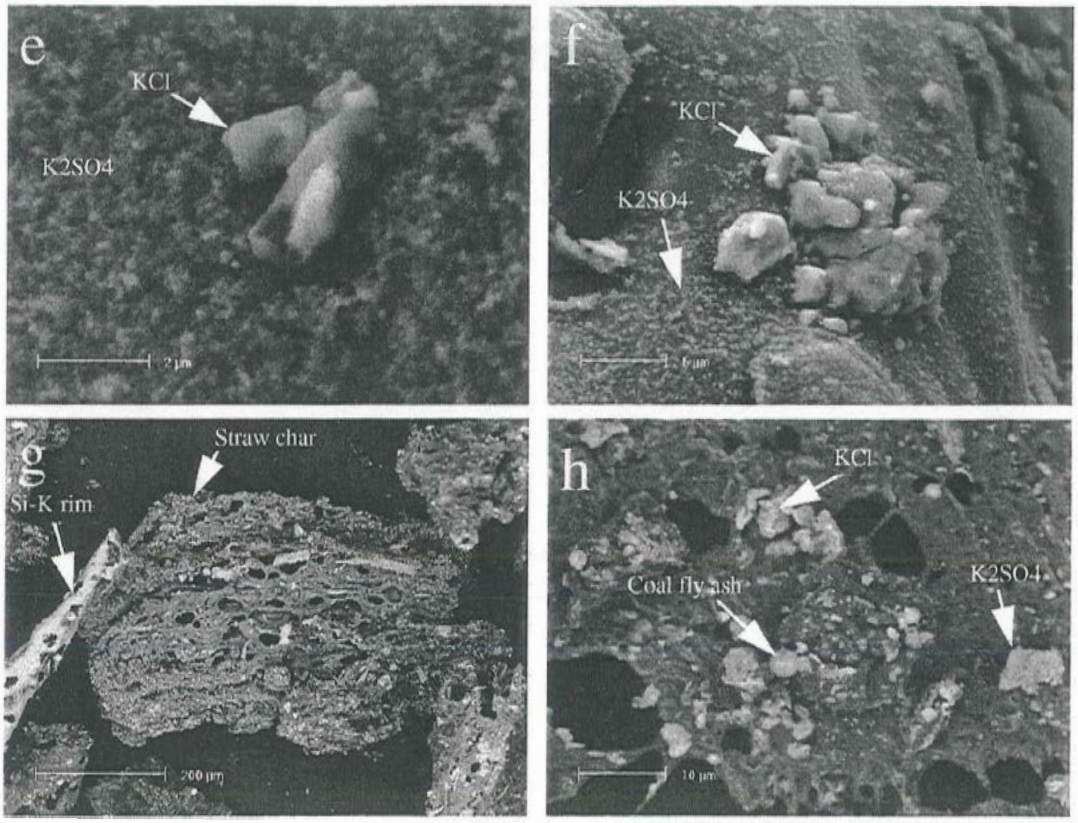

Fig.3.8e-h. Representative BSE images of char powder samples (experiment 2, 20% straw, 75% load).

e) High magnification BSE image showing 2 micron KCl crystals and coating of K_2SO_4 on a Si-K rich rim.

f) Aggregate of KCl crystals and partial coating of K_2SO_4 on Si-K rich rim.

g) Interior of straw char showing the highly porous structure that is formed during degassing of the straw. Also seen is a broken off Si-K rim.

h) Shows detail of straw char interior. Attached to the organic structure are K_2SO_4, KCl and a spherical coal-derived fly ash.

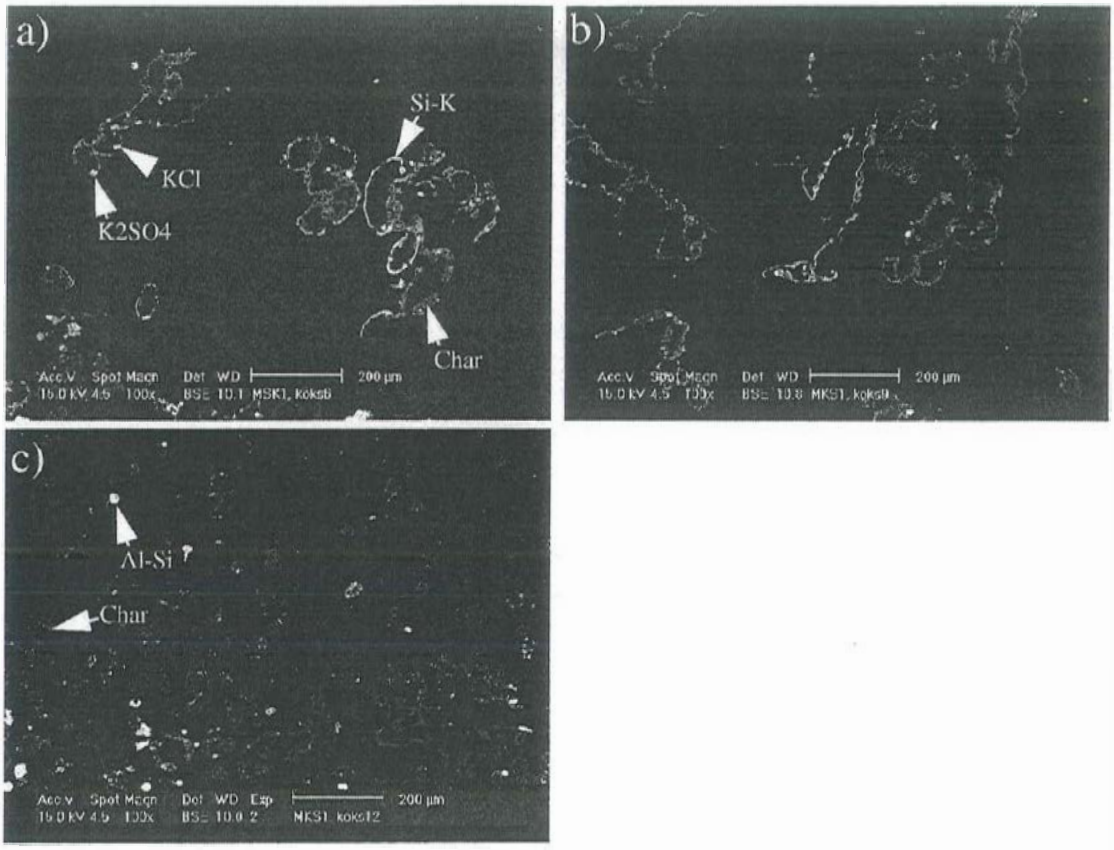

Fig.3.9. BSE images of embedded and polished chars.

a) Char from exp.2: 20% straw, 75% load. b) Char from exp.4: 10% straw 100% load, c) char from exp.9: 100% coal, 100% load. The straw chars in a) and b) illustrate the Si-K rich rims as well as attached KCl and K_2SO_4. c) The image shows only coal chars illustrating their smaller size and rounded morphology compared to straw chars.

3.5.1. Summary of chars from MKS1

The straw chars are typically covered or partially covered with fragile appearing Si-K rich rims. Attached to the rims are small KCl and sometimes K_2SO_4 crystals and a thin appearing K_2SO_4 coating covers much of the rim surface. The observations indicate that KCl and K_2SO_4 have condensed on the Si-K compound either in the flame zone or during sampling. During sampling the flue gas continually flows past the collected, cooled chars and through the filter. Therefore condensation on the chars is likely to occur during this process. Coal chars are typically smaller and rounded compared to the elongated straw chars. Occasionally coal derived fly ash particles are attached to the straw chars, but condensed KCl or K_2SO_4 were not observed on coal chars. This feature indicates that some (perhaps the initial) condensation occurred in the flame zone,

because otherwise one would expect coal and straw chars to exhibit similar amounts of KCl and K_2SO_4.

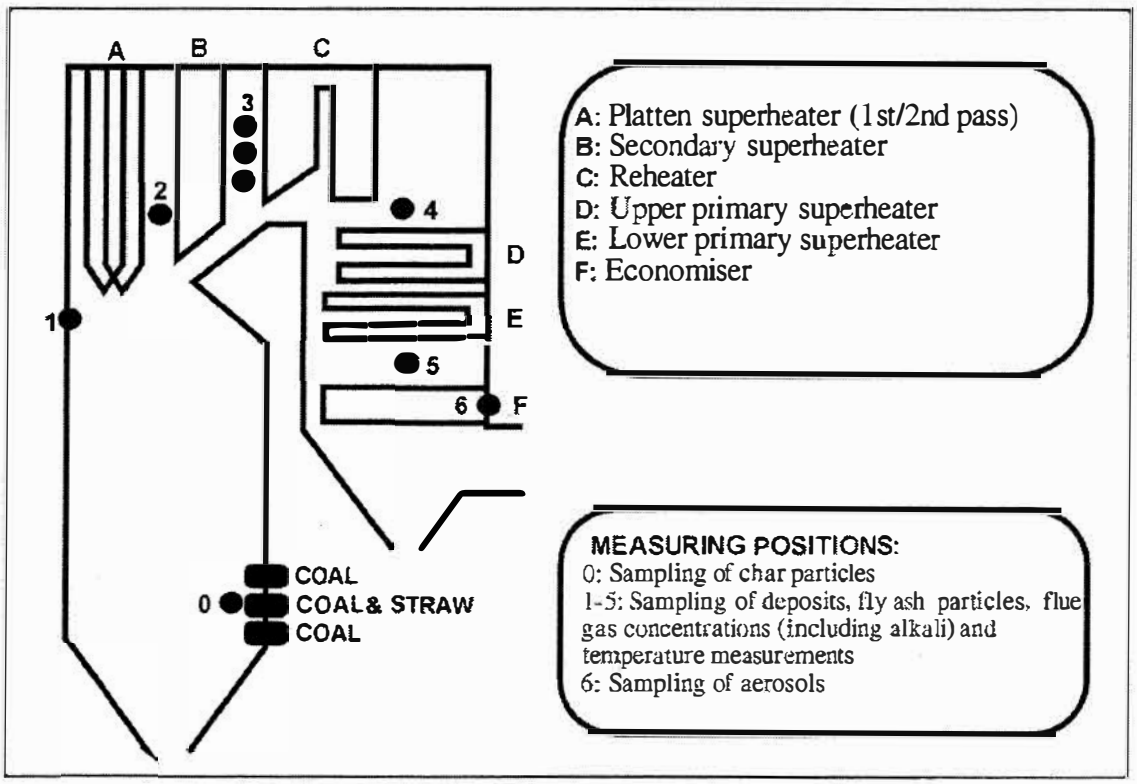

Fig.3.10. Schematic illustration of the MKS1 boiler at Studstrupværket. Filled circles indicate deposition probe locations (modified after Andersen et al., 1997).

3.6 Full scale ashes from MKS1, Studstrupværket

Fly ash and bottom ash from MKS1, Studstrupværket were subjected to CCSEM analysis (section 4.5). The study was concentrated on bottom ash and fly ash from experiments 3, 4 and 5, all with 100% load and 20%, 10% and 0% straw addition, respectively. The bottom ash was collected dry once every hour, whereas the fly ash was collected in an electrostatic filter. Figure 3.10 illustrates schematically the MKS1 boiler design. Representative images of bottom ash and fly ash samples are shown in Fig.3.11.

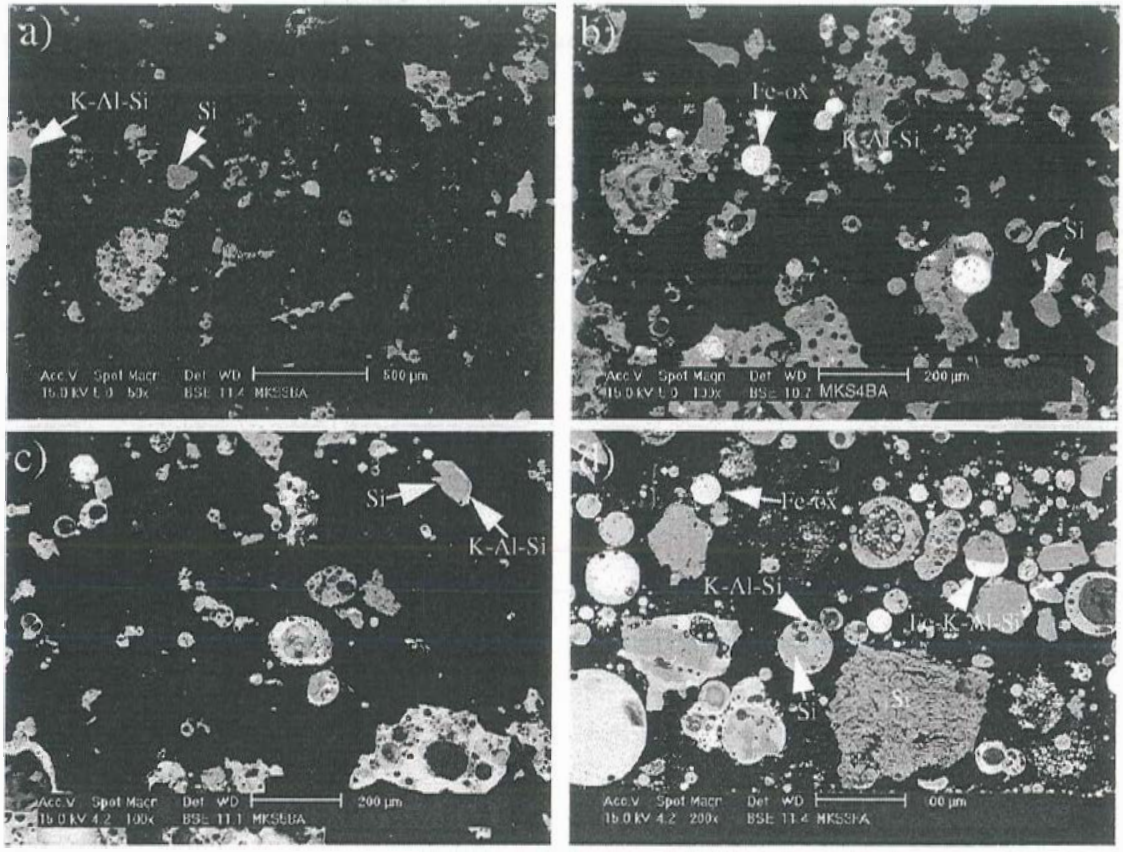

Fig.3.11a-d. Bottom ash and fly ash samples fromMKS1.

a) Bottom ash from experiment 3 (MKS3BA); b) Bottom ash from experiment 4 (MKS4BA); c) bottom ash from experiment 5 (MKS5BA); d) fly ash from experiment 3 (MKS3FA).

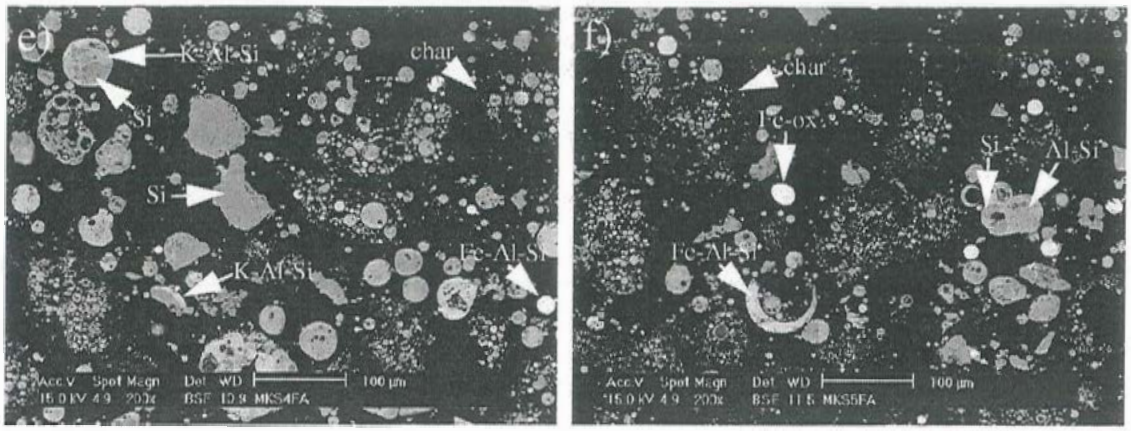

Fig.3.11e-f. Bottom ash and fly ash samples from MKS1 (continued).

e) fly ash from experiment 4 (MKS4FA); f) fly ash from experiment 5 (MKS5FA).

The bottom ash samples (a-c) all contain a high proportion of relatively large (up to 300 micron) particles that are mainly composed of Si with various amounts of other elements such as Al, K, Ca and Fe. The particles generally appear amorphous and fused. Commonly they contain vesicles and many are composite being composed of domains of both pure Si and various alumino-silicates. In the samples from co-combustion (MKS3BA and MKS4BA) it is not uncommon to observe rims of alumino-silicates with a substantial content of K and Ca surrounding Si-rich cores.

The fly ash samples (d-f) contain many spherical fused particles that are composed mainly of K-(Ca-Fe) bearing alumino-silicates. Additionally silica-rich particles are prominent and amorphous composite particles consisting of both phases are commonly observed. The alumino-silicates in the fly ash sample without straw addition (MKS5FA) contain less K than the two with 20 and 10% straw addition.

3.6.1. Comments to the bottom ash and fly ash images.

The bottom ash and fly ash particles from MKS 1 are strongly dominated by various silica-rich particles. Of special interest is the observation of K-containing alumino-silicate particles or rims surrounding cores of almost pure silicon in the experiments with straw addition. Due to the fluxing effect of K on silica-rich compounds their presence will most likely have an adverse effect on deposit formation due to a lower melting point and thereby higher sticking propensity. Clearly, in the case of zoned particles the composition at the margin is quite important for the stickiness of a particle.

3.7 Deposits from MKS1, Studstrupværket

Five deposits from MKS1 were analyzed by Scanning Electron Microscopy Point Counting (SEMPC) to evaluate their composition as function of straw addition and location in the boiler and to compare them to fly ashes. Schematic location of the deposit probes is illustrated in Fig.3.10. The deposits and the associated straw fractions and loads are presented in Table 3.2. The analyzed deposits were all exposed for 18 hours with a probe metal temperature of 540°C. All SEMPC analyses were performed on the upstream deposit, i.e. the position pointing towards the direction of the gas flow.

Table 3.2. Deposit samples selected for SEMPC analysis.

Code	Straw	Load	Position
MKS31D-1	20%	100%	1
MKS32D-1	20%	100%	2
MKS33D-1	20%	100%	3
MKS41D-1	10%	100%	1
MKS42D-1	10%	100%	2
MKS51D-1	0%	100%	1

After exposure the probes were embedded in epoxy and cross sectioned, ground and polished with the final step being 0.25 micron diamond spray. Before SEM analysis the blocks were coated with a thin carbon layer. The SEMPC analyses were performed by setting up a number of adjoining frames at 200 times magnification covering part of the upstream deposit. In each of the frames 20 by 20 points were set up in a grid and analyses were performed at each point. Care were taken to analyse the whole thickness of the deposit. It was unavoidable to overlap a small part of the probe metal when setting up the areas (Fig.3.12). To avoid inclusion of probe metal in the data treatment results with Cr_2O_3 > 0.1 % (w/w) were omitted from the dataset. However, some of the oxidized metal-layer may be incorporated in the data treatment. To avoid analyzing epoxy filled pores data collection was stopped if the total counts were below 600 after 1 second. The remaining X-ray spectra were quantified using theoretical standards included in the EDX-system. Figure 3.12 shows examples of upstream deposits that were subjected to SEMPC. The thin bright zone at the top of each image shows the probe metal that is overlapped by analysis.

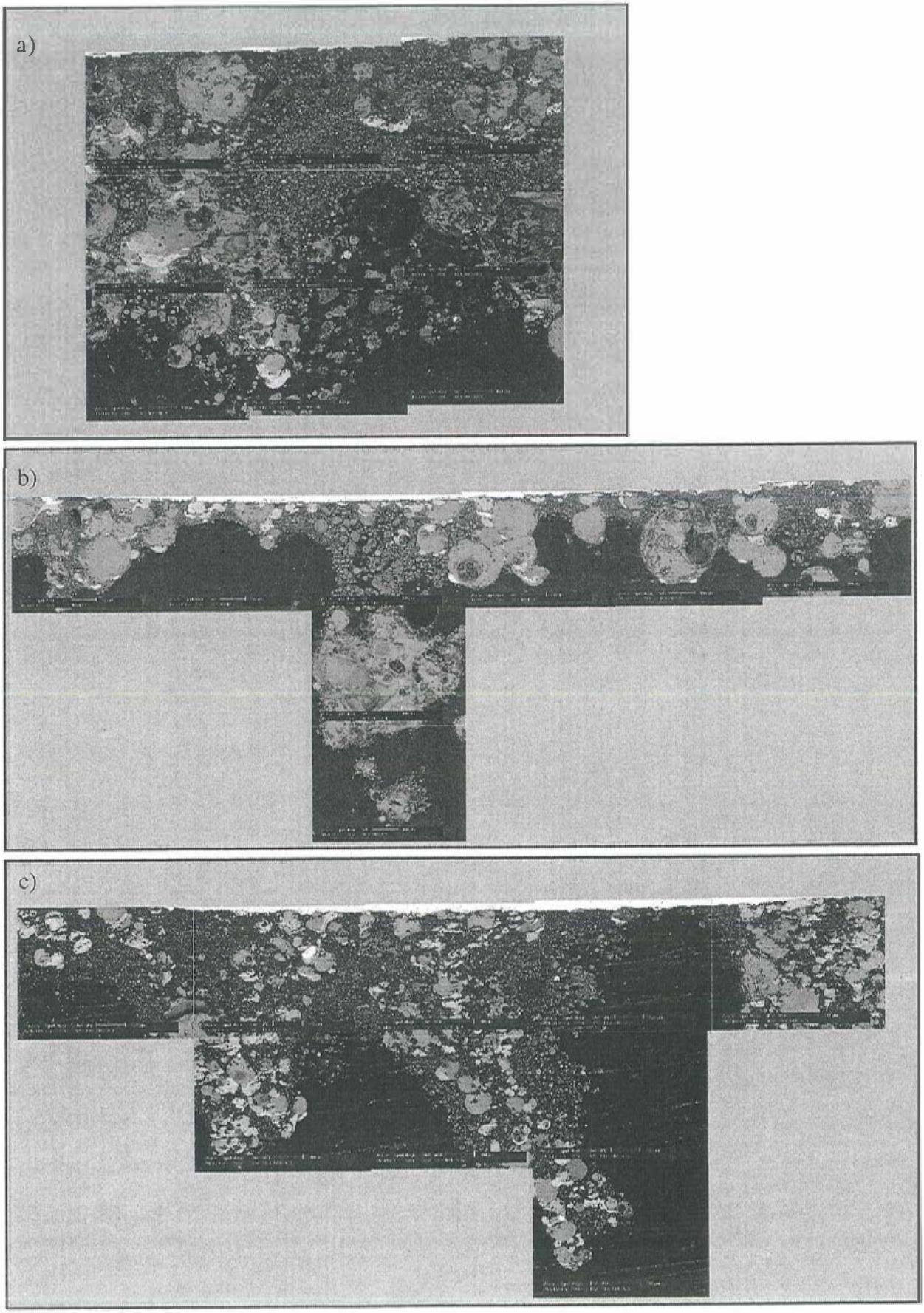

Fig.3.12. Examples of deposit sections used for SEMPC.

Fig. 3.12. (preceeding page). Examples of deposit sections used for SEMPC.

a) Deposit MKS32D-1, upstream (experiment 3, 20% straw, position 2, 540°C metal temperature, 18 hours exposure). The image consists of 9 individual 200x magnification photomicrographs. The deposit is approximately 1.2 mm thick on average with an undulating surface. It appears that the presence of large particles coincide with "hills" whereas small particles coincide with "valleys" on the surface.

b) Deposit MKS42D-1, upstream (experiment 4, 10% straw, position 2, 540°C metal temperature, 18 hours exposure). The image is put together of 8 individual 200x magnification photomicrographs. The deposit was formed in the same position as in a) but with only 10% straw addition compared to 20%. The deposit varies in thickness between 100 micronto 1.2 mm and is strongly undulating.

c) Deposit MKS51D-1, upstream (experiment 5, 0% straw, position 1, 540°C metal temperature, 18 hours exposure). The image is put together of 9 individual 200x magnification photomicrographs. The deposit varies in thickness from 0 to 1.3 mm in a "finger-like" structure. Again it seems that the outward extending fingers coincide with relatively large particles.

The SEMPC technique yields no information of particle size or distribution. Therefore an X-ray mapping of a selected superheater deposit was performed to illustrate these features (Fig.3.13). The brightness on the map is proportional to the intensity of the X-ray energies assigned to each element. The X-ray mapping shows that K_2SO_4 is largely present as a binding phase covering the surfaces of fly ash particles.

Fig.3.13. (following page). X-ray mapping of MKS32D-1, upstream. The Si mapping illustrates the presence of Si-rich fly ash particles. Evidently fly ash particles with no or low Si are also present. These are mainly rich in Fe. The mapping of K and S reveals their correlation in thin coatings and zones in between fly ash particles. This indicates that K_2SO_4 constitutes a binding phase of this superheater deposit. The frame furthest to the left shows a backscatter image for reference.

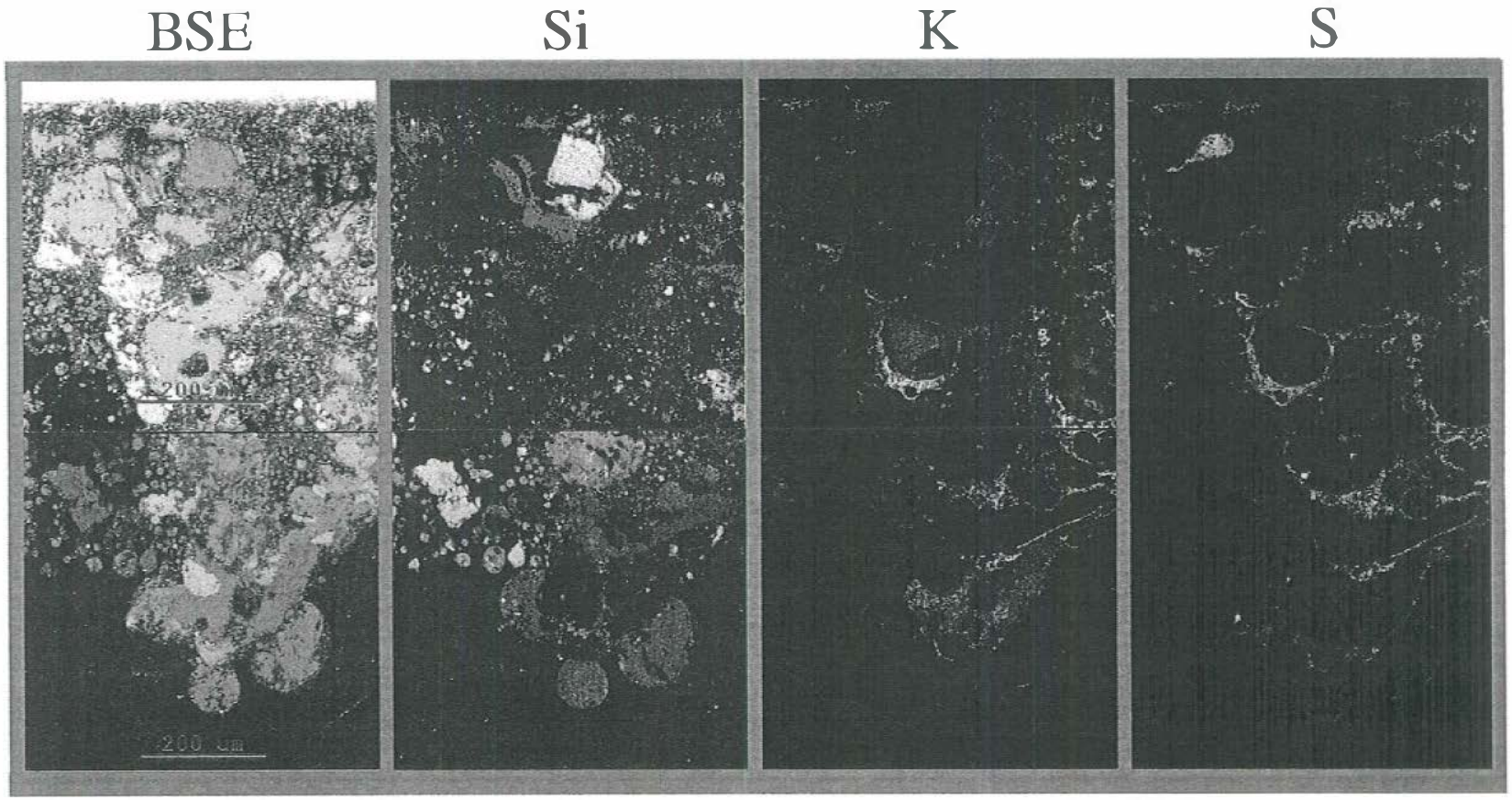

Fig.3.13. X-ray mapping of MKS32D-1, upstream superheater deposit.

3.8 Laboratory ashes

Fuels were ashed at dK-Teknik in order to study similarities and differences between laboratory ashes and full scale ashes and to assess the extent to which laboratory ashing may assist in predicting ash deposition problems. In this section a number of representative BSE-images of laboratory ashes are shown.

3.8.1 Ashed danish wheat straw and wheat grain

As examples of two biomass fuels of contrasting compositions wheat straw and wheat grain were ashed at dK-Teknik. The samples were ashed at both 550°C and 815°C to test the consequence of different ashing temperatures for the produced ash. Representative BSE images are shown in Fig.3.14.

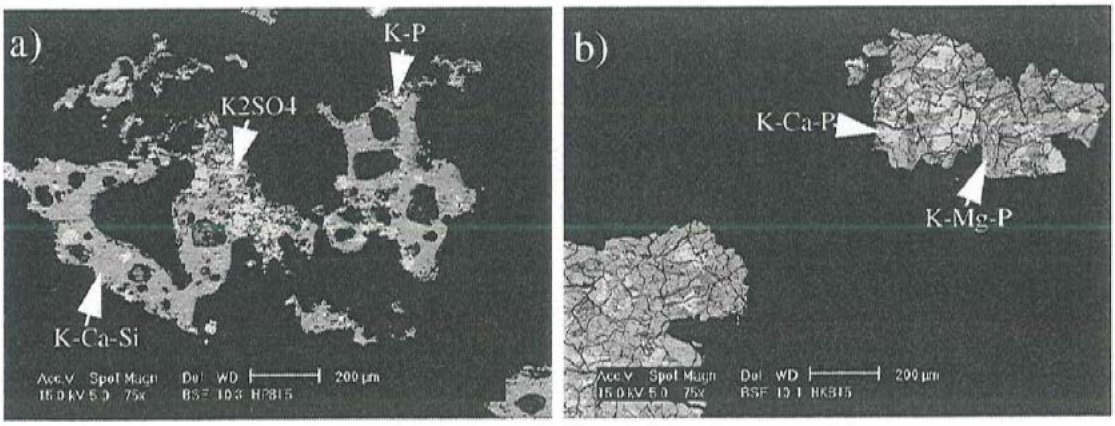

Fig.3.14a-b. Wheat straw and wheat grain high-temperature (815°C) laboratory ashes.

a) Wheat straw ashed at 815°C. The ash consists of strongly fused, vesicular amorphous particles up to millimeter size. The particles are mainly composed of K-Ca silicate with subordinate K-phosphates and K-sulphates.

b) Wheat grains ashed at 815°C. The ash consists of fused particles reaching up to several mm in size (not shown).The particles contain various phosphate phases, the brightest being rich in K and Ca, whereas the darker areas are rich in K and Mg. Regular grain margins suggest that the particles have recrystallized into these compounds.

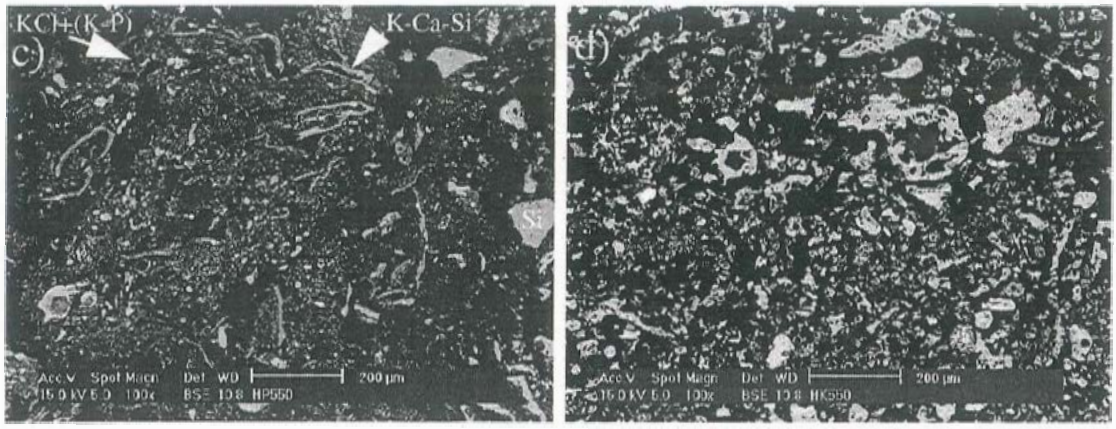

Fig.3.14c-d. Wheat straw and wheat grain low-temperature (550°C) laboratory ashes.

c) Wheat straw ashed at 550°C. The sample consists partly of sub-micron to micron-size particles of KCl and K-phosphate and partly of larger K-Ca silicates either occurring as elongated rims or as equant grains. Morphologically the laboratory ash is quite similar to the full scale fly ash samples shown in Fig.3.4. However, the laboratory ash typically contain a smaller amount of KCl than straw fly ash. This can partly be a result of evaporation of some Cl during the laboratory ashing even at this relatively low temperature, but is mainly believed to be a consequence of element fractionation between bottom ash and fly ash, so that the fly ash is relatively enriched in KCl (see section 4.3.1).

d) Wheat grains ashed at 550°C. The ash particles vary in size from around 5 micron to 250 micron. As was the case for the 815°C ash, the particles consist mainly of various phosphates rich in K with subordinate Mg and Ca.

3.8.1.2. Comments to the straw and grain laboratory ashes

The ashes that were produced at 815°C are strongly fused and consist of massive slags. Based on morphology they are therefore very unlike fly ash. Also taking into account that volatile components as for example Cl and K evaporates to a significant extent this high temperature is not considered viable for producing ashes to be utilized for fusion or sintering experiments. In contrast ashing at 550°C produces particulate straw ash that morphologically appears similar to full scale fly ash as observed in the Haslev and Slagelse samples.

3.8.2 Ashed wheat straw, coal and fuel blends from MKS1 at Studstrupværket

Fuels (coal and straw) and mixed fuels (80% coal, 20% straw on an energy basis) from MKS 1 experiment 3 were ashed in the laboratory at dK-Teknik. Additionally, coal from experiments 4 and 5 were ashed. Coals were ashed at 815°C whereas straw and straw-

coal mixtures were ashed at 550°C to minimize evaporation of alkalies. All laboratory ashes were analyzed by CCSEM (section 4.6) and representative BSE images of the ashed samples are shown i Fig. 3.15.

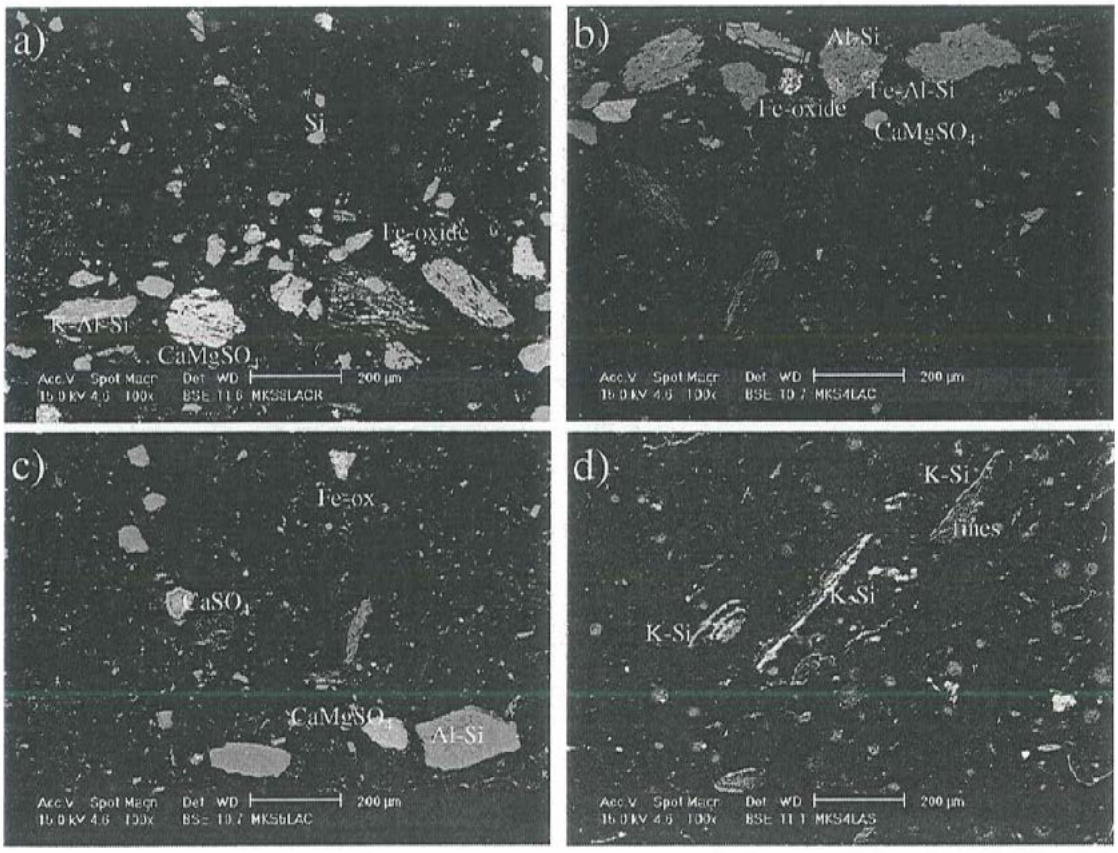

Fig.3.15a-c. Laboratory ashes from MKS1.

a) MKS3LAC. 815°C coal ash, experiment 3. The image shows various alumino-silicates, Ca-Mg sulphates and Fe oxides. The sample is relatively coarse grained with particles extending in size up to around 200 micron. The fine-grained particles consist mainly of Al-Si rich material.

b) MKS4LAC 815°C coal ash, experiment 4. The image is dominated by coarse particles of various alumino-silicates, Ca-Mg sulphates and Fe oxide. The diffuse dark grey, round structures that are present are pieces of an acrylic filler that were mixed in to keep ash particles from touching each other.

c) MKS5LAC. 815°C coal ash from experiment 5. The image illustrates various alumino-silicates, Fe-oxide, Ca sulphate and Ca-Mg sulphate.

d) MKS3LAS. 550°C ash of wheat straw from experiment 3. The image shows thin elongate particles that are primarily composed of K and Si. Attached to these are typically masses of fine grained material composed of mixtures of K, Ca, Mg, S, Cl and P. These particles are too small to be analyzed individually.

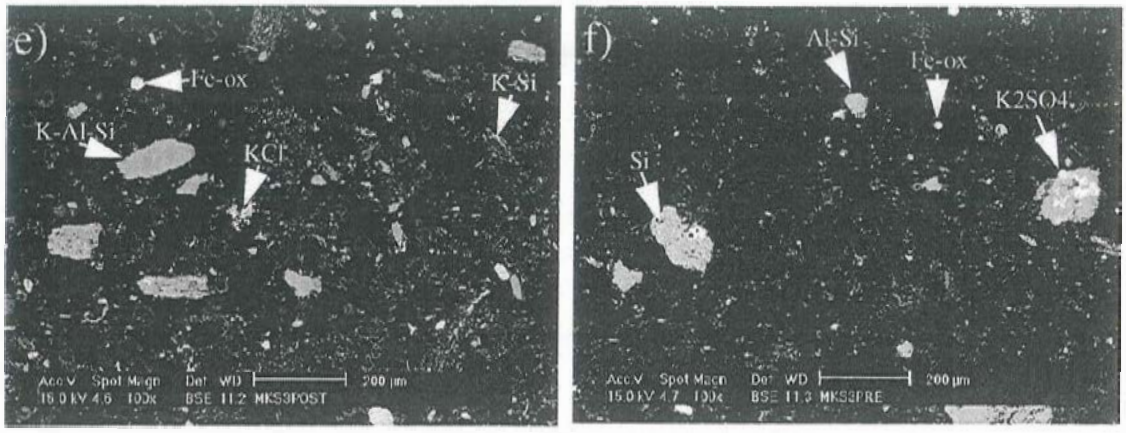

Fig.3.15e-f. Laboratory ashes from MKS1.

e) MKS3POSTMIX. This sample is a blend of coal laboratory ash and straw laboratory ash (i.e. MKS3LAC and MKS3LAS). The ashes are mixed to represent 20% straw addition on an energy basis. The sample is dominated by the coal ash (alumino-silicates and sulphates) wheras only a few K-Si rich flakes are evident. The sample was prepared by physically mixing the two ashes after the ashing process.

f) MKS3PREMIX. The sample was prepared by first blending straw and coal and subsequently ashing the mixture at 550°C. The most significant difference to MKS3POSTMIX is the presence of K_2SO_4 and the apparent lack of KCl.

3.8.2.1 Comments to MKS1 laboratory ashes

The coal ash samples are dominated by relatively large particles of alumino-silicates, quartz, Ca-Mg sulphates and minor Fe oxide. Fine-grained material is largely composed of silica-rich compounds. Straw ash on the other hand is mainly composed of elongated flakes of K-Si rich particles that morphologically resemble flakes of similar composition that are observed in straw chars (Fig.3.9). Masses of fine-grained material are typically composed of mixtures of K, Ca, Mg, Cl, S and P. The particles in these masses are generally too small to be analyzed individually. Fine-grained material is also seen lying freely in the embedding epoxy. The physically mixed ash (MKS3POSTMIX) is dominated by the coal ash. From the presence of K_2SO_4 in MKSPREMIX it appears that K reacts with S preferentially to Cl, the S being supplied by the coal.

4. CCSEM results

In this section the results from the CCSEM analyses are presented and discussed. Results from Haslev CHP and Slagelse CHP are treated in Sørensen (1997) and Hansen et al. (1997), and therefore only the main findings from these power plants will be discussed. Results from MKS1 are reported in Frandsen et al. (1998a). The full set of CCSEM and SEMPC data are presented in Frandsen et al. (1998b).

4.1. CCSEM analysis

The proceedures for sample preparation are descibed in section 3. The use of CCSEM analysis for characterization of minerals in coal and coal ash at GEUS has recently been described in detail by Laursen (1997a; 1997b) and therefore only the basics of the technique will be mentioned here:

1. A number of points is set up randomly to cover a large part of the sample surface. At each point an analysis is performed at three different magnifications (25x, 100x and 500x) to achieve good resolution in the whole size range.
2. A Backscatter Electron (BSE) image with a good separation between inorganic and organic material is acquired at each point.
3. An appropiate grey-level threshold value is set to create a binary image with only inorganic particles singled out.
4. The binary image is used to control the beam to perform a scan across each particle for five seconds. A particle is here defined as any cluster of connecting white pixels in the binary image.
5. An energy-dispersive X-ray spectrum and morphological data are acquired during each scan yielding coupled compositional and morphological data for each particle.

It shall be stressed that the CCSEM results are semi-quantitative for several reasons:

1. The EDX spectrum is not corrected for ZAF effects (Z: atomic number, A: absorbtion and F: fluorescence).
2. Particle size is based on cross sectional area and weight percent is estimated on the assumption that all particles are spherical. This involves an uncertainty for non-spherical particles.
3. Particles with average diameters below 1 micron are omitted from the CCSEM analysis because much of the detected X-rays are emitted from a volume beyond the particle boundary, potentially leading to erroneous results.
4. Organically bound or otherwise disseminated elements are not detected by the CCSEM method which only "sees" particles with high BSE reflection, i.e. inorganic or inorganic-rich particles.

These aspects are, however, not critical for the CCSEM analysis because the X-ray spectra are primarily used to group particles into mineral categories with rather wide ranges of composition. The strength of a CCSEM analysis lies in information about element distribution between different particle types and different samples and in the fact that each particle is characterized with respect to both size and composition. However, it is emphasized that a CCSEM analysis is not directly comparable to a traditional bulk chemical analysis.

The raw X-ray data are used to group the analyzed particles into a number of categories, commonly called mineral categories. However, it must be appreciated that the categories are only defined by composition and bears no information on crystallinity. The principles of data reduction are described in Laursen (1997a) and Sørensen (1997).

The strategy for modifying the CCSEM technique to be suited for analysis of straw ashes was to obtain an elaborate set of CCSEM raw data on ashes from Slagelse CHP and Haslev CHP and subsequently to utilize them to develop a new data reduction algorithm. In total 12 ashes were analyzed by CCSEM. Initially the raw data were reduced by using coal mineral characterization algorithms developed by Laursen (1997a). Due to the contrasting composition of straw ash and coal ash this resulted in a high number of unclassified particles (35-70%), i.e. particles that do not fit the criteria for any of the mineral categories. The compositions of the unclassified particles were subsequently studied in detail, and it was found that particles rich in chlorine and

sulphur constituted a significant part pointing to the importance of chlorides and sulphates, compounds that have been reported to be present in biomass ashes elsewhere (e.g. Olanders and Steenari, 1994; Steenari and Langer, 1988; Bryers, 1994). In the case of wheat grains the unclassified fraction is dominated by particles rich in P (K, Mg and Ca rich phosphates).

On the basis of semi-quantitive SEM/EDX analysis and corresponding ratios between X-ray intensities a number of new categories were established in order to characterize the ash particles more complete. After each modification of the algorithms the datasets were categorized again and the amount of unclassified particles were taken as a measurement of the success of the algorithm.

Modifications of the algorithm included addition of a number of new categories. A composite category of KCl associated with silicates (KCl+silicate) were included, an association that is commonly observed in especially fly ash samples. These composite particles either represent Si-rich particles with condensated KCl or they result from close association between KCl and silicate induced during sample handling and preparation (Fig.3.4). Such adjoined particles are seen as one single particle by a CCSEM analysis which yields an "average" composition" with characteristics from the involved phases.

A category of particles rich in K, Ca and Si called "K-Ca silicate" were included in the algorithm. Characteristic for this category is a very low Al-content in contrast to what is the case for clay-derived particles originating from soil. The K-Ca silicates can form by reaction between silica from the straw and vaporized inorganic species in the flue gas. Some of the K-Ca silicates, however, may have formed by reaction between volatilized inorganic species and quartz grains. Additionally, categories for K_2SO_4 and KCl were included in the algorithm as these phases constitute significant parts of especially the fine fly ash fractions. A range of phosphates: K phosphate, Ca phosphate and K-Mg phosphate were included in order to encompass ash particles derived from wheat grain.

The unclassified group were subdivided into unclassified phosphates, -sulphates, -chlorides and -silicates on the basis of their contents of P, S, Cl and Si, respectively.

This subdivision was based on the assumption that particles belonging to these groups will respond differently to high temperatures. Most of the categories from the coal mineral algorithms were retained and their proportions were observed to be practically unaltered compared to the initial data-reduction. This is important for future comparison between CCSEM analyses of coal ash and straw ash and especially for CCSEM analysis of ash from co-combustion of straw and coal. As mentioned earlier, the categorization is based only on chemical composition and do not contain crystallographic information. Hence, a categorization as for example quartz only implies that a particle has a composition with >80% Si and <10% Al on a count ratio basis (Table 4.1), and does not imply that the mineral quartz is present.

The modification of the algorithms resulted in a decrease in the proportion of unclassified to between 4% and 25% for bottom ash from wheat and barley straw, whereas fly ash contained between 6% and 27% unclassified. In the case of rape straw, which were included in the analyses, unclassified still constituted 63% of the fly ash, underlining that it is problematic to encompass ash from biomass with contrasting compositions into one datareduction algorithm. The algorithm presently used is tuned to characterize ash from combustion of wheat and barley straw as well as ashes from co-combustion of straw and coal. Table 4.1 shows the algorithm that is presently used for characterization of ash from straw and from co-combustion of straw and coal.

Table 4.1. Data reduction algorithms for ashes and deposits from straw combustion and co-combustion of straw and coal.

quartz:	Al <= 10, Si >= 80
iron oxide:	Mg <= 5, Al <= 5, Si < 10, S <= 5, Fe >= 80
periclase:	Mg >= 80, Ca <= 5, S <= 5
rutile:	S <= 5, Ti >= 80
alumina:	Al >= 95
calcite:	Mg <= 5, Al <= 5, Si <= 5, P <= 5, S < 10, Ca >= 80, Ti <= 5
dolomite:	Mg >= 5, Ca > 10, Mg + Ca >= 80
ankerite:	Mg < Fe, S < 15, Ca > 20, Fe > 20, Ca + Mg + Fe > 80
kaolinite (Al-Si):	Na <= 5, K <= 5, Ca <= 5, Fe <= 5, Al + Si >= 80, (0.8*Al) < Si, Si < (1.5*Al)
montmorrillonite (Ca-Al-Si):	Na <= 5, K <= 5, Ca <= 5, Fe <= 5, Al + Si >= 80, (1.5*Al) < Si, Si < (2.5*Al),
illite (K-Al-Si):	Na <= 5, Ca <= 5, Fe <= 5, Al >= 15, Si > 20, K > 5, K + Al + Si >= 80,
Fe-Al silicate:	Na <= 5, Al >= 15, Si > 20, K <= 5, Ca <= 5, Fe > 5, Fe + Al + Si >= 80
Ca-Al silicate:	Na <= 5, Al >= 15, Si > 20, K <= 5, Ca >= 5, Ca + Al + Si >= 80, Fe <= 5
Na-Al silicate:	Na >= 5, Al >= 15, Si > 20, Na + Al + Si >= 80, K <= 5, Ca <= 5, Fe <= 5
aluminasilicate:	Na <= 5, Al > 20, Si > 2, Si + Al >= 80, K <= 5, Ca <= 5, Fe <= 5
mixed silicate:	Na < 10, Al > 20, Si > 20, K < 10, Ca < 10, Fe < 10, Na + Al + Si + K + Ca + Fe >= 80
Fe silicate:	Na <= 5, Al <= 5, Si > 20, S <= 5, K <= 5, Ca <= 5, Fe > 10, Fe + Si >= 80
Ca silicate:	Na <= 5, Al <= 5, Si > 20, S <= 5, K <= 5, Ca > 10, Ca + Si >= 80, Fe <= 5
Ca aluminate:	Al > 15, Si <= 5, Ca > 20, Ca + Al >= 80
pyrite:	S > 40, Ca < 10, Fe >= 10, Fe + S >= 80, Fe <= (S * 0.7)
pyrrhotite:	Fe + S >= 80, Fe > 20, S > 20, (0.7*S) < Fe, Fe < (1.5*S), Ca < 10
gypsum:	Si < 10, S > 20, Ca > 20, Ca + S > 80, Ti < 10, P <= 5
apatite:	Al <= 5, P >= 20, S <= 5, Ca >= 20, Ca + P >= 80
Ca-Al phosphate:	Al > 10, Si <= 5, P > 10, S <= 5, Ca > 10, Al + P + Ca >= 80
KCl:	K >= 30, Cl >= 20, K + Cl >= 70
K_2SO_4:	K >= 30, S >= 20, K + S >= 70
K phosphate:	K >= 35, P >= 30, K + P >= 70
K-oxide/hydroxide:	K >= 90
Ca phosphate:	Ca >= 30, P >= 30, Ca + P >= 70
K-Mg phosphate:	K >= 25, Mg >= 15, P >= 20, K + Mg + P >= 80
NaCl:	Na >= 30, Cl >= 30, Na + Cl >= 80
K-Ca silicate:	Si >= 20, Si <= 80, K + Ca >= 25, Al <= 2
Si-rich:	Si >= 65, Si <= 80, S <= 10, P <= 10, Cl <= 10
Ca-rich:	Al < 15, Ca >= 65, Ca <= 80, P <= 10, S <= 10, Cl <= 10
Ca-Si-rich:	Si >= 20, Ca >= 20, Si + Ca >= 70, S <= 10, Cl <= 10, P <= 10
KCl+silicate:	K >= 20, K >= (0.9 * Cl), K <= (1.7 * Cl), Si >= 15
unclassified silicate:	Si > 20, S <= 5, P <= 5, Cl <= 5
unclassified sulphate:	S >= 20, S <= 5, P <= 5, Cl <= 5
unclassified chloride:	Cl >= 20
unclassified phosphate:	P >= 20
unclassified:	remaining particles

4.2. Danish wheat straw, wheat grain and laboratory ash

CCSEM analyses were performed on examples of two biomass fuels to evaluate the technique for characterization of inorganic elements in biomass. The results are given on a mineral category basis together with results for 550°C laboratory ashes in Table 4.2.

CCSEM analyses of wheat straw and grain show that the inorganic fraction differs strongly from what is usually observed in coal. Clay-minerals and pyrite, which are both important mineral constituents in coal, only constitute insignificant proportions of the detected inorganic particles in straw and grain. The most important categories in the

analysed straw are quartz, various phosphorous - and chlorine rich phases as well as potassium-sulphate. The quartz-category is believed primarily to be present as amorphous SiO_2 x nH_2O, an opal-like compound that is common in cereals (Marschner, 1995). In contrast, the analysed wheat grains have a distinctly different association of inorganic particles, being dominated by phosphorous-rich phases with subordinate quartz (Table 4.2). The phosphorous-rich particles are mainly phytates, which function as nutrient storage for the grains (Fig.3.1b) (Marschner, 1995).

Table 4.2. CCSEM results on a weight percent category basis

Category	Wheat straw	Straw lab.ash 550°C (LAS1)	Wheat grain	Grain lab.ash 550°C (LAG1)
Apatite (Ca-P)	1.6		2.1	
K_2SO_4	3.6	3.2		
Ca silicate	2.0		3.2	
Ca-rich	2.6		1.0	
Calcite	2.4		2.8	
Dolomite	1.2			
K-phosphate				94.4
K-Al silicate	1.3			
K-Ca silicate		39.3		
K-Mg phosphate			42.7	
KCl		14.5		
KCl+silicate		2.6		
Quartz	52.0	6.0	10.8	1.7
Si-rich	1.6		0.5	
Unclassified chloride		2.5		
Unclassified phosphate	6.7	1.9	23.1	1.0
Unclassified silicate	4.2		5.0	
Unclassified sulphate	1.2			
Unclassified	13.6	26.1	4.3	1.1
Sum	94.0	96.1	95.5	98.2

Only categories that constitute more than 1 % (w/w) are shown.

The level of K and Cl detected in the straw is quite low taken into account that these elements are important constituents of untreated straw. The cause of this is that the CCSEM technique only detects that part of the inorganic material that is present in distinct inorganic particles, i.e. low-concentration disseminated or organically bound elements are not analysed. To assess the content of disseminated inorganic elements a number of SEM/EDX analyses were performed on areas without any inorganic particles, revealing less than 0.2% K_2O and below 0.25% Cl on a weight basis. Concentrations at these levels are too low to allow quantification by SEM/EDX,

meaning that dispersed elements in the organic structure can be detected but not quantified by SEM/EDX.

Wheat straw and wheat grains were ashed in the laboratory at 550°C. The CCSEM results show that there is a marked compositional difference between the ash from straw and grain, respectively (Table 4.2). The grain ash is dominated by K (Mg, Ca)-phosphates in accordance with the phosphorous-rich composition of the inorganic portion of the grains. In contrast, the straw ash is dominated by silicates, KCl and minor K_2SO_4 and unclassified chlorides. The high content of silicates is expected due to the high content of the quartz category in the straw. The silicates in the ash, however, are mainly K-Ca silicates with a low Al-content, in contrast to silica-rich ash particles formed during coal-ashing, which (except for quartz) generally are rich in Al. The K-Ca silicate particles are believed to have formed during the ashing by reaction between organically dispersed K and Ca with remains of the straw-derived silica. This assumption is supported by the CCSEM results which show that the straw mineral fraction contains more than 50% of the quartz category and no K-Ca silicates, whereas the low temperature ash contains only 6% quartz and 39% K-Ca silicate (Table 4.2). KCl constitutes 14% of the laboratory ash whereas this category was not detected in the straw fuel, indicating that much of the KCl is mainly formed from dispersed K and Cl during the ashing process. Alternatively, KCl crystals in the straw are too small (< 1 micron) to be detected by CCSEM analysis.

4.3. Haslev CHP and Slagelse CHP

The CCSEM study was focused on bottom ash and fly ash. Additionally, fuel from Haslev 1 and deposits from Slagelse 3 and Haslev 1 were analyzed. A short description of the sampling procedures are given in section 3.2 and BSE images are shown in sections 3.2.1 and 3.2.2. The CCSEM study of straw ashes and deposits from the Haslev and Slagelse Combined Heat and Power Plants (CHP) is additionally reported in detail in Sørensen (1997) and Hansen et al. (1997). In Sørensen (1997) the modification of the CCSEM technique to be suited for straw ash characterization is discussed in detail, while comparison between CCSEM results and ash fusion as determined by

Simultaneous Thermal Analysis (STA) (Hansen, 1997) and High Temperature Light Microscopy (HTLM) (Hjuler, 1997) is discussed in Hansen et al. (1997).

4.3.1. Bottom ash and fly ash from straw fired plants: Haslev CHP and Slagelse CHP

The CCSEM results of the bottom ash and fly ash from the 6 experiments are shown in Table 4.3 and illustrated in pie-diagrams in Fig. 4.1.

Table 4.3. CCSEM results for ashes from Haslev CHP and Slagelse CHP presented as weight percent on a category basis.

Sample:	HAS1BA	SLA1BA	SLA3BA	SLA6BA	SLA7BA	SLA8BA	HAS1FA	SLA1FA	SLA3FA	SLA6FA	SLA7FA	SLA8FA
Fuel:	wheat	wheat	barley	wheat	wheat	rape	wheat	wheat	barley	wheat	wheat	rape
K_2SO_4	1.0						1.1		1.7		1.0	8.3
Ca-rich												9.5
Ca-Si-rich			1.1			1.4						
K-Al silicate	1.1				1.3	1.0	1.4				1.1	
K-Ca silicate	34.1	30.0	83.8	79.3	58.7	67.9	14.8	4.2	2.2	1.0	4.0	10.9
KCl	2.3			1.8			26.9	39.2	62.1	85.0	58.3	2.5
KCl+silicate							8.4	19.9		6.5	11.4	1.1
Quartz	32.2	47.0	5.2	5.5	19.9	11.0	17.1	12.4			4.4	
Si-rich	19.4	20.7	5.5	9.0	15.7	11.3	8.5	4.9			3.5	1.6
Uncl. chloride							3.5	4.5		1.4	3.9	
Uncl. silicate	1.3		1.2				1.2					
Uncl. sulphate							1.0					1.7
Unclassified	5.1		2.1	1.7	1.3	4.3	13.8	11.6	26.9	3.7	10.4	60.3
Sum	96.5	97.7	98.9	97.2	96.9	97.0	97.8	96.7	92.9	97.7	98.0	95.8

Only categories that constitute more than 1 % (w/w) are shown. The suffix BA signifies bottom ash whereas the suffix FA signifies fly ash.

The bottom ashes are typically rich in silica-rich categories, especially K-Ca silicate, quartz and Si-rich. Only minor KCl is present and K_2SO_4 is only detected in HAS1BA. The unclassified category constitutes less than 5% in the case of wheat and barley combustion and only 4% in the case of rape combustion. In contrast, the fly ashes are generally rich in KCl and KCl+silicate and have a rather low but variable content of K-Ca silicates. In the fly ash K_2SO_4 is present in minor quantities except in the case of rape fuel (SLA8FA) where it constitutes 8%, reflecting that rape is rich in sulphur compared to wheat and barley. The unclassified category constitutes between 4% and 14% in the case of wheat combustion, 27% for barley and 60% for rape combustion, illustrating that the data reduction algorithms are primarily suited to fly ash from wheat and barley combustion. Hence, in the case of a fuel of contrasting composition such as rape, a high amount of unclassified particles remain.

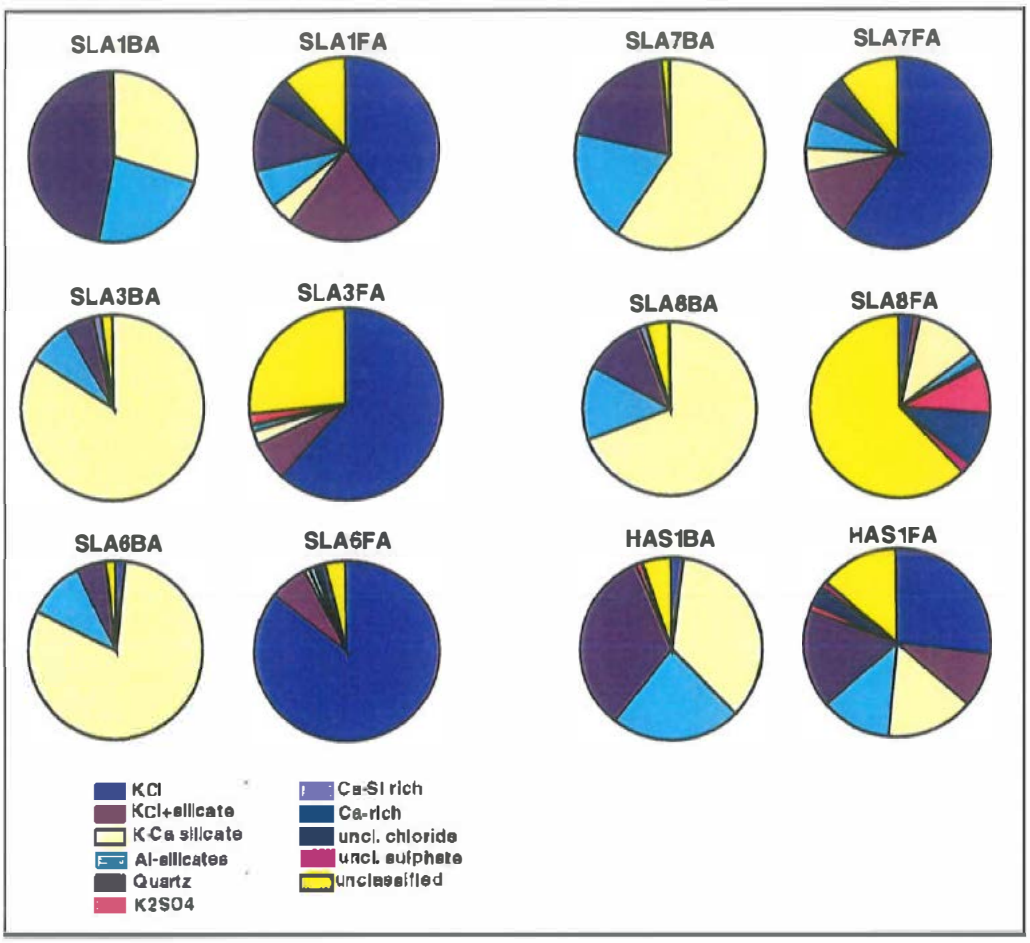

Fig.4.1. Pie diagrams of fly ash and bottom ash from Haslev CHP and Slagelse CHP.

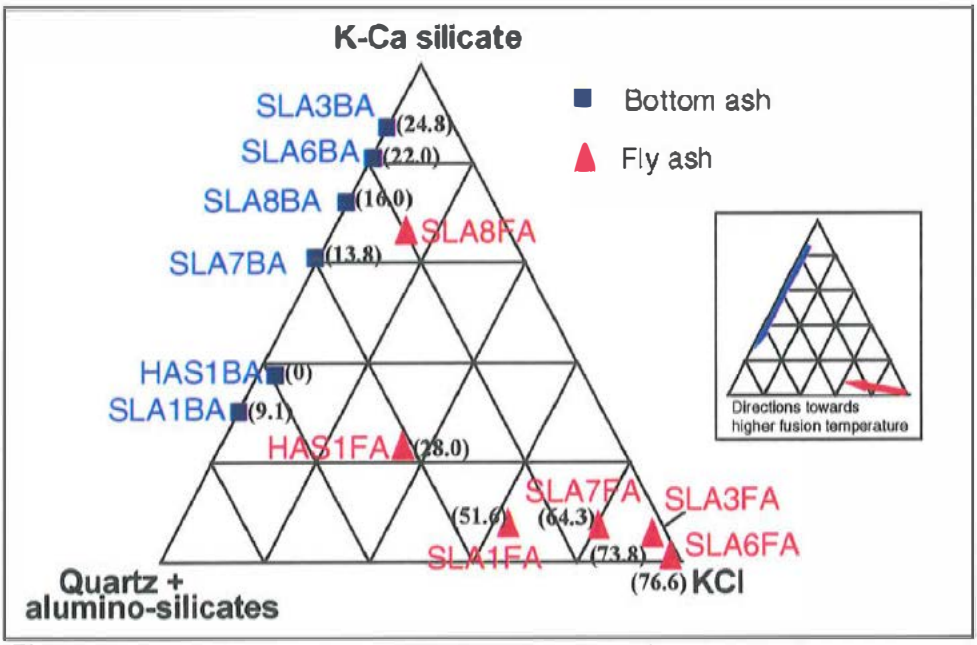

Fig. 4.2. Fly ash and bottom ash samples from Haslev and Slagelse experiments represented in triangular diagram of selected categories. The numbers in brackets indicate the melt fraction at 880°C as measured by STA analysis (Hansen et al., 1997).

To illustrate the variations in composition and in an attempt to correlate category composition with melting behaviour of straw ashes, the results are plotted in a triangular diagram of KCl, K-Ca silicates and quartz+alumino-silicates (Fig.4.2). The group of alumino-silicates consists of Ca-Al silicates, Fe-silicates, Fe-Al silicates, Si-rich, K-Al silicates, Al-silicates, mixed silicate and unclassified silicates. These are categories which are believed mainly to be derived from terrigeneous dust. The quartz category, however, is mainly believed to be derived from the straw but can additionally be in the form of included quartz grains. The three end-members constitute more than 90% of the bottom ashes and more than 60% of the fly ashes with the exception of rape fly ash (16%). The basis for creating this type of diagram is that it is expected that the melting of the ash will correlate with position due to the contrasting melting temperatures of the end-members. KCl melts at 770°C whereas K-Ca silicates may melt at temperatures as low as around 740°C if present in eutectic proportions [Morey et al., 1931]. However, most of the K-Ca silicate particles have compositions in the range of 5-15% CaO, 70-85% SiO_2 and 10-25% K_2O as illustrated in the three dimensional triangular diagram in Fig. 4.3. These compositions will begin to melt at the eutectic temperature, but the major part will, under equilibrium conditions, not melt until higher temperatures have been reached. The group of "quartz+alumino-silicates" will clearly have a wide range of melting temperatures, but it is assumed that in general the melting will occur at higher temperatures than for K-Ca silicates. This is especially true of the quartz category which on its own will not melt until 1713°C (Deer et al., 1966). Separation between bottom ash and fly ash is distinct in the triangular diagram of KCl - K-Ca silicates - quartz+alumino-silicates (Fig.4.2). Bottom ash is situated close to the silicate baseline, whereas fly ash range from close to the KCl apex roughly towards a ratio of 85% "quarts+aluminosilicates" and 15% K-Ca silicates. This indicates that the silicate association in the fly ash generally has a lower ratio of material formed by reaction between silica and gas alkalies (K-Ca silicates) than what is observed in the bottom ash. The location of SLA8FA (rape fly ash) is not considered in this discussion since only 16% of the total is accounted for in the diagram. By comparison with ash fusion tests by STA it was shown that ash fusion correlates well with position in the diagram. In Fig.4.2 the numbers in brackets indicate the melt fraction at 880°C for the

Slagelse ashes, and a consistent trend of relatively high melt fractions close to the apexes of KCl and K-Ca silicate in contrast to low melt fractions close to the apex of quartz+various alumino-silicates is observed. A further discussion of position in this type of diagram in relation to fusion data is presented in Hansen et al. (1997).

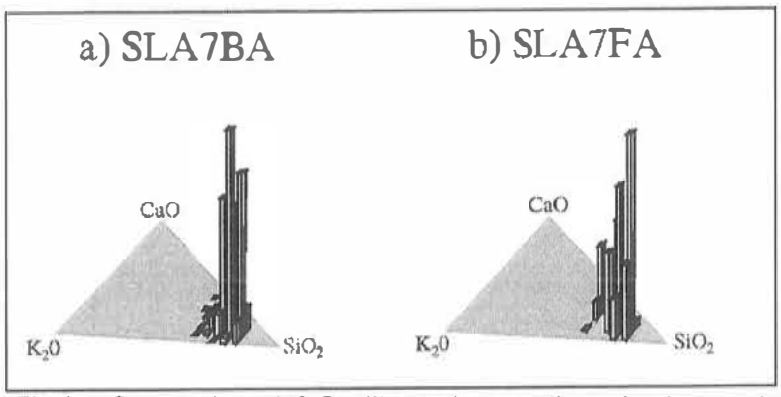

Fig.4.3. Composition of K-Ca silicates in three-dimensional triangular diagrams. The relative heights of the columns indicate the cumulative weight percent.

4.3.2. Deposits sampled at the Haslev 1 and Slagelse 3 experiments.

Deposits were sampled on water cooled deposition probes both in the furnace and the superheater region of the Haslev and Slagelse boilers. For probe positions and sampling procedures see section 3.3 and Fig. 3.5. The CCSEM results for the Haslev deposits are presented together with a fly ash analysis for comparison in Table 4.4.

Table.4.4. CCSEM results for fly ash and deposits from Haslev 1.

Category	HAS1FA	HAS1SD-1	HAS1SD-2	HAS1FD-1	HAS1FD-2	HAS1FD-3
K_2SO_4	1.1	1.8				
Ironoxide						2.2
K-Al silicate	1.4					
K-Ca silicate	14.8	3.8	1.1	28.9	19.8	2.3
KCl	26.9	76.0	80.8	61.1	71.2	76.6
KCl+silicate	8.4	3.0	6.1	1.6	2.6	7.7
Quartz	17.1	1.0				
Si-rich	8.5					
Unclassified chloride	3.5	4.4	6.6	1.3		4.6
Unclassified phosphate				2.7		
Unclassified silicate	1.2					
Unclassified sulphate	1.0	1.2	1.4			
Unclassified	13.8	4.9	3.0	3.0	3.6	6.3
Sum	97.8	96.7	99.0	98.59	97.1	99.6

Only categories that constitute more than 1 % (w/w) are shown. HAS1FA: fly ash; HAS1SD-1 and HAS1SD-2: outer superheater deposit; HASFD-1 and HASFD-2: outer furnace deposit; HAS1FD-3: inner furnace deposit.

Figure 4.4 shows the average composition with respect to chlorides (KCl+unclassified chloride), KCl+silicate, K-Ca silicates and quartz+ Si-rich, of the respective deposit-types and fly ash. The content of K-Ca silicate is significantly higher and chlorides a bit lower in the outer (loose) furnace deposit than in the inner (hard) deposit. The Fe-oxide in the inner part of the furnace deposit (Table 4.4) probably reflects parts of the oxidized probe metal surface that were detached during brushing off the deposit. The outer superheater deposit is similar to the inner part of the furnace deposit in terms of chloride and K-Ca silicate content.

The results indicate that in the furnace deposition of KCl by condensation is most important in formation of the inner deposit, whereas fly ash particle impaction is a dominating process for formation of the outer part. Additionally, it appears that condensation of KCl is more important in the superheater region than in the furnace. When comparing the deposits in general to the fly ash it is seen that the deposits are all higher in chlorides and lower in quartz than the fly ash. Additionally, it is seen that the silicate fraction changes from being dominated by quartz to be dominated by K-Ca silicates when going from fly ash to deposits, indicating that reaction between K and silicates continues during and after deposit formation.

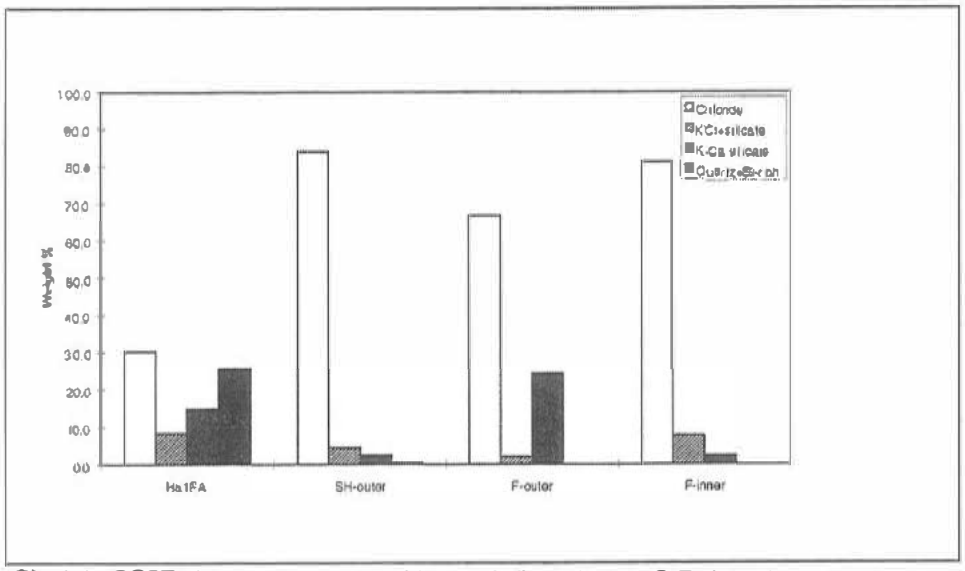

Fig.4.4. CCSEM category compositions of fly ash (HASIFA) and average compositions for outer superheater deposit (SH-outer), outer furnace deposit (F-outer) and inner furnace deposit (F-inner).

CCSEM results for the analyzed Slagelse 3 deposits are shown together with a fly ash analysis for comparison in Table 4.5. Figure 4.5 shows the average composition with respect to chlorides (KCl+unclassified chloride), KCl+silicate, K-Ca silicates and quartz+Si-rich, of the respective deposit-types and fly ash. The inner deposit from the furnace probe is depleted in K-Ca silicates and enriched in KCl as well as KCl +silicate compared to the outer (loose) bulk sintered deposit part.

Table 4.5. CCSEM results for fly ash and deposits from Slagelse 3.

Category	SLA3FA	SLA3SD-1	SLA3SD-2	SLA3SD-3	SLA3FD-1	SLA3FD-2	SLA3FD-3
K_2SO_4	1.7			1.4			
Iron oxide				1.2			
K-Ca silicate	2.2		4.6	2.1	68.1	68.1	28.0
KCl	62.1	96.1	89.1	83.4	18.1	2.5	35.6
KCl+silicate				1.6			5.0
Quartz						1.0	
Unclassified chloride				1.1			6.2
Unclassified silicate						1.1	
Unclassified	26.9	2.6	4.4	6.1	12.8	24.8	23.4
Sum	92.9	98.6	98.1	97.0	99.1	97.4	98.2

Only categories that constitute more than 1 % (w/w) are shown. SLA3FA: fly ash; SLA3SD-1 and SLA3SD2: outer superheater deposit; SLA3SD-3: inner superheater deposit; SLA3FD1 and SLA3FD-2: outer furnace deposit; SLA3FD-3: inner furnace deposit.

This indicates that the inner (initial) furnace deposit is formed primarily from condensation of KCl whereas for the outer part, which contains a large fraction of silicates, impaction of fly ash particles played a more dominant role. Both the inner and outer deposits from the superheater probe contain more chloride than is the case for the inner furnace deposit, indicating that deposit formation by KCl condensation is more important in the superheater than in the furnace, substantiating the results from Haslev 1. The fly ash sample is notably low in silicate-rich particles and rich in KCl, being quite similar to the superheater deposits.

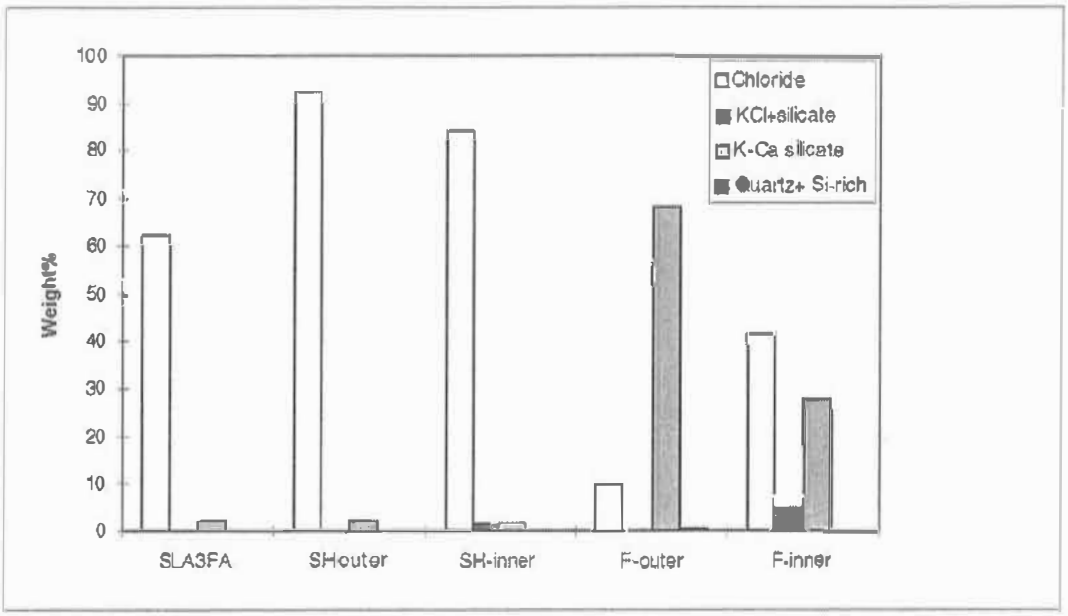

Fig.4.5. CCSEM category compositions of fly ash (SLA3FA) and average compositions of outer superheater deposit (SH-outer), inner superheater deposit (SHinner), outer furnace deposit (F-outer) and inner furnace deposit (F-inner).

4.4 Co-combustion of straw and coal at MKS1, Studstrupværket, char samples.

Various samples were obtained from MKS1 at Studstrupværket. This section deals mainly with CCSEM results for chars that were sampled in the burner zone where straw and coal were mixed. The objective was to acquire a snapshot of the conditions present at an intermediate stage of combustion between raw fuel and ash. Chars were sampled at three experiments burning 20%, 10% and 0% straw, respectively (MKS2CH, MKS4CH and MKS9CH). BSE-images of chars are shown in Figs.3.8 and 3.9 and results of the CCSEM results for chars are shown in Table 4.6. The samples consist of both straw chars and coal chars so the results represent a mixing of inorganic components of both types.

There are quite large variations in the CCSEM composition between the three samples. The differences can to a large extent be accounted for by varying proportions of coal char and straw char in the sample. Therefore the main discussion is concerned with the differences between char from coal-alone combustion on one side (MKS9CH) and chars from straw+coal combustion on the other side (MKS2CH and MKS4CH) (Fig.4.6). The compositional variations between chars from the two straw+coal fired

experiments probably mainly reflect local variations in the straw-coal ratio at the exact sampling location rather than variations in the overall straw fraction. Chars from coal combustion are rich in various Al-silicates (a grouping of all alumino-silicates except K-Al silicate) compared to co-combustion chars. Otherwise the main differences are that K_2SO_4 and other sulphates (unclassified sulphates) as well as KCl are present in high amounts in co-combustion chars and not in coal chars. As discussed in section 3.5.1 these two phases are to a large extent believed to be condensed on the chars during sampling. However, their presence substantiates that some K, Cl and S are vaporized during the initial degassing phase.

Table 4.6. CCSEM results on a category basis for MKS1 chars.

Category	MKS2CH	MKS4CH	MKS9CH
Alumino-silicate			6.4
Ca-P		1.8	
K_2SO_4	11.9	23.2	
Fe-Al silicate			6.8
K-Al silicate (Illite)	16.6	7.6	7.6
K-Ca silicate	2.3	1.6	
Al-Si (kaolinite)	3.4		18.8
KCl	7.6	8.1	
Ca-Al-Si (montmorrillonite)	1.6		16.3
Pyrite			1.2
Quartz	31.7	24.3	25.9
Si rich	3.9	5.5	
Unclassified phosphate		2.0	
Unclassified silicate	4.2	1.9	10.0
Unclassified sulphate	1.2	8.4	1.3
Unclassified	8.5	10.6	1.3
Sum	93.0	94.8	95.6

Only categories that constitute more than 1% (w/w) are shown.

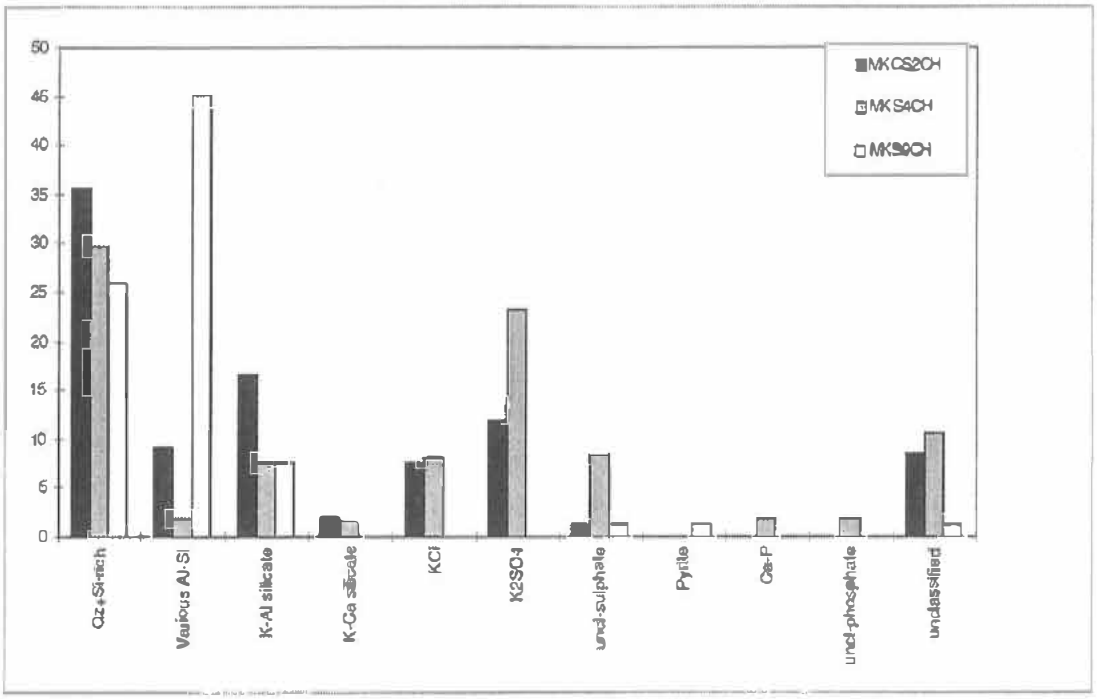

Fig.4.6. Schematic illustration of composition by selected categories for MKS1 chars. MKS2CH: 20% straw; MKS4CH: 10% straw; MKS9CH: coal.

4.5 Co-combustion of straw and coal at MKS1, Studstrupværket, ash samples.

Fuel coal, bottom ash, fly ash and deposits from MKS1 were analysed by CCSEM. The study was concentrated on three experiments in order to investigate the influence of increasing the straw proportion as shown in Table 4.7. The samples were kindly provided by Karin Hedebo Andersen and are part of a major measurement and sampling campaign at MKS1 (Andersen et al., 1997). The full CCSEM dataset is given in Frandsen et al. (1998a) and the data are discussed in detail in Frandsen et al. (1998b, Appendix G). A summary of important observations and results concerning the element distribution in bottom ash and fly ash is given in this section, with reference to fuel and deposit results.

Table 4.7. List of parameters for experiments 3, 4 and 5 at MKS1, Studstrupværket.

Exp. no.	Code	Straw share	Load
3	MKS3	20%	100%
4	MKS4	10%	100%
5	MKS5	0%	100%

The CCSEM results for bottom ashes and fly ashes from the three experiments are given in Table 4.8. This section is specially concerned with the distribution of K_2O in the ashes, since the utilized wheat straw contains significant amounts of easily vaporized potassium that can cause slagging and fouling problems. No significant phosphates - or chlorides of potassium were detected in the analysed ashes, which are strongly dominated by silica-rich phases (Table 4.8). The two silicate-categories which are richest in K_2O are illite (actually ash-particles with composition similar to illitic clay) and mixed silicate. On average the illite category contain between 3.5 and 6.0% K_2O and mixed silicate contain between 2.0 and 4.7% K_2O (w/w) based on CCSEM analysis. The remaining silicate categories typically contain significantly less K_2O.

Table 4.8. CCSEM results on a category basis for MKS1 bottom ash and fly ash.

Category	MKS3FA	MKS4FA	MKS5FA	MKS3BA	MKS4BA	MKS5BA
Alumino-silicate	5.8	5.1	10.6	3.0	11.0	21.8
Ca silicate	1.5					
Ca-Al silicate	1.5	2.	2.2	3.8	4.7	3.5
Ca-Si-rich	1.9					
Fe-Al silicate	3.2	2.7	9.0		2.7	7.6
Dolomite			1.2			
Illite	30.4	33.6	7.8	22.7	22.0	1.7
Kaolinite	1.7	7.6	13.9			2.1
Mixed silicate	1.9	1.2	2.1	2.2	2.9	
Montmorrilonite	4.5	7.8	32.0	1.3	1.9	8.1
Na-Al silicate		2.4				
Quartz	17.9	14.0	4.3	21.8	22.3	23.3
Si-rich	7.0	3.8		26.7	8.7	4.9
Unclassified silicate	19.0	14.3	11.2	13.5	17.7	25.6
Unclassified	1.6	2.4	2.1	1.3	1.4	

Only categories that constitute more than 1% (w/w) are shown.

In Fig. 4.7 the contents of illite+mixed silicate is compared to the total content of other alumino-silicate phases and quartz in ashes from the three experiments. In both the fly ashes and the bottom ashes the content of the K_2O rich silicates (illite and mixed silicate) are relatively high and similar in the two experiments with straw addition (MKS3 and MKS4) and significantly lower in MKS5 in which coal alone were utilized. For fly ash the content is lower by a factor of ca. 3 and for the bottom ashes the content is lower by a factor of ca. 12. In contrast the content of other alumino-silicates are similar and relatively low in the straw+coal tests and relatively high in the coal-alone

test. The quartz category appear to increase with straw addition in the case of the fly ashes, whereas it is roughly constant in the bottom ashes.

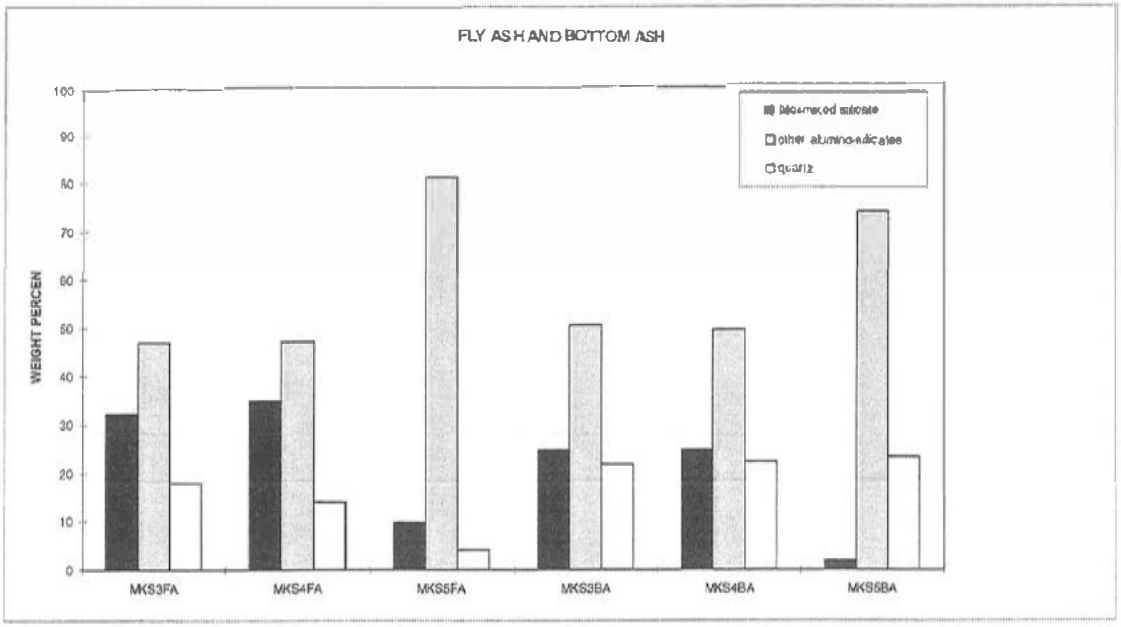

Fig.4.7. Selected category groups in fly ash and bottom ash from experiments 3, 4 and 5.

Fly ash from experiments 3, 4 and 5 are plotted in three-dimensional triangular diagrams of SiO_2-K_2O-Al_2O_3 in Figure 4.8. The height of the columns are proportional to the relative weight percent of particles in the compositional range defined at the basal plane. In the case of coal combustion (MKS5FA) two major peaks are noticed, one composed of virtually pure SiO_2 and one located on the SiO_2-Al_2O_3 line. The first peak represents quartz-derived particles whereas the second represents clay-derived particles. In both cases of straw addition (MKS4FA and MKS3FA) there is a relative increase in the SiO_2 peak compared to in MKS5FA, indicating that straw-derived SiO_2 is preferentially incorporated in the fly ash. Notably the clay-derived peaks in MKS3FA and MKS4FA are moved towards the K_2O apex of the diagram compared to MKS5FA. This relative increase in K_2O in the silicate particles is in agreement with the changes in category composition with straw addition that were shown in Fig. 4.7.

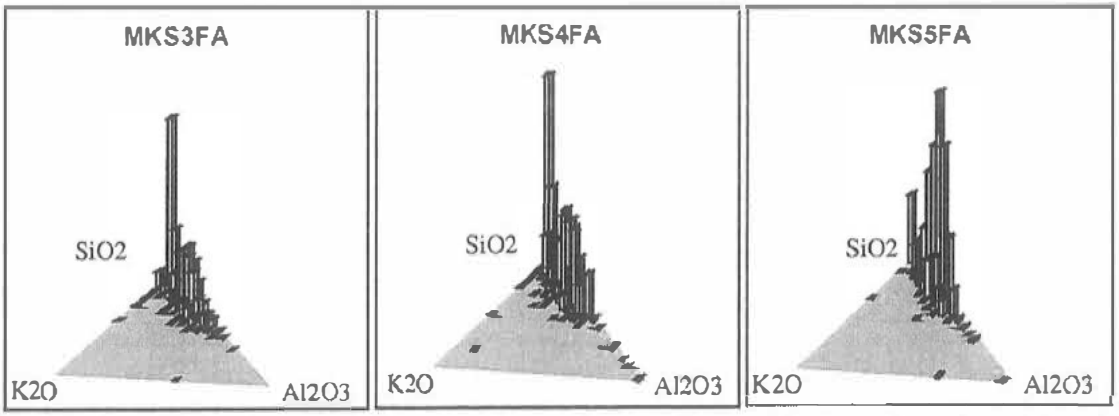

Fig.4.8. CCSEM data for fly ash from experiments 3, 4 and 5 plotted in three-dimensional triangular diagrams of SiO_2-K_2O-Al_2O_3.

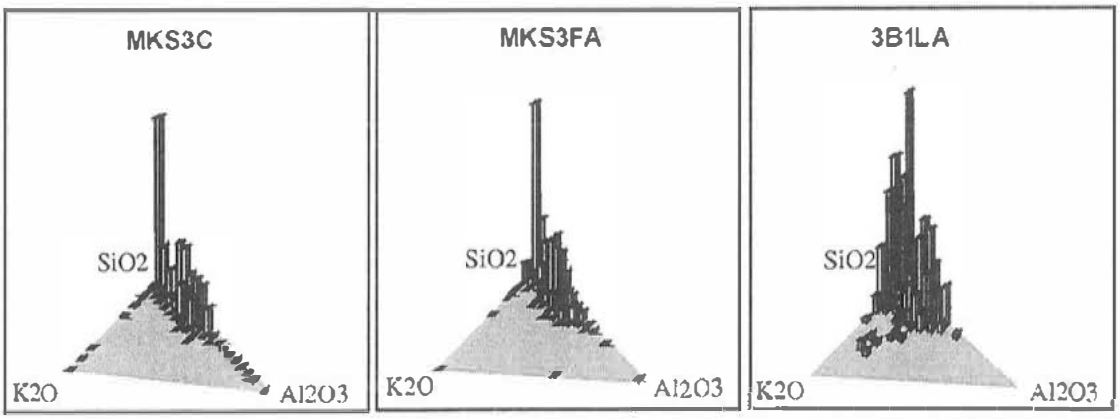

Fig.4.9. Three-dimensional triangular diagrams of SiO_2-K_2O-Al_2O_3 for coal minerals (MKS3C), fly ash (MKS3FA) and superheater probe deposit (3B1LA) from experiment 3 at MKS1. The deposit 3B1LA were analyzed by SEMPC, whereas MKS3 and MKS3FA were analyzed by CCSEM.

In Fig.4.9 the relative K_2O content is shown for coal, fly ash and an upstream deposit from position 1 in MKS3 (20% straw). It appears that during the conversion from coal minerals to fly ash there is a slight but significant increase in relative content of K_2O as evidenced by a slight movement of the columns towards K_2O. This trend is even more evident when going from fly ash to the superheater deposit in which the K_2O content is significantly higher compared to what is the case for both coal minerals an fly ash. The increase in K_2O from coal minerals to fly ash is explained by reaction between alumino-silicates from the coal and vaporized potassium from the straw. The change from fly ash to deposit composition is explained by continuing potassium - alumino-silicate reaction and additionally to formation of $K\ SO_4$ (see also section 3.7, Fig.3.17).

4.5.1. Discussion of CCSEM results for ashes from MKS1

The data strongly suggest that straw-derived K_2O to a large extent reacts with, and is incorporated in, coal-derived alumino-silicates. The data do, however, not show any clear linear correlation between straw share and K_2O enrichment. Rather the levels are similar in the two experiments with straw addition differing from the case of coal alone.

The quartz category increases with straw addition in the fly ash whereas it is relatively constant in the bottom ash, indicating that straw derived SiO_2 preferentially ends up in the fly ash. It is suggested that remains of the silica straw-skeleton upon dehydration and ashing largely are present as minute flake-like particles which are easily carried by the gas flow.

During the measurement campaign at MKS1 no severe deposit problems were encountered with increasing the straw share up to 20% (Andersen et al., 1997). The data presented above show that straw derived K_2O to a large extent is captured by coal-derived alumino-silicate particles, a feature which was also qualitatively observed in SEM images (Figs.3.2, 3.3 and 3.4). No significant KCl or K_2SO_4 were formed in the ashes. However, K_2SO_4 was observed in the superheater probe deposit in the case of 20% straw share. It is suggested that the K_2O capture by the alumino-silicates provides an efficient alkali-binding, which deters slagging and fouling processes as long as the fusion temperature is not lowered critically by the fluxing effect of alkali on the silica phases.

4.6. Ashed wheat straw, coal and mixtures of wheat straw and coal from MKS1 at Studstrupværket

Laboratory ashes of MKS1 fuels were analyzed by CCSEM to evaluate what consequence "premixing" or "postmixing" has on resulting ash composition (see explanation below). Five laboratory ashes were produced as schematized in Fig.4.10 and representative BSE images of the ashes are shown in Fig.3.15.

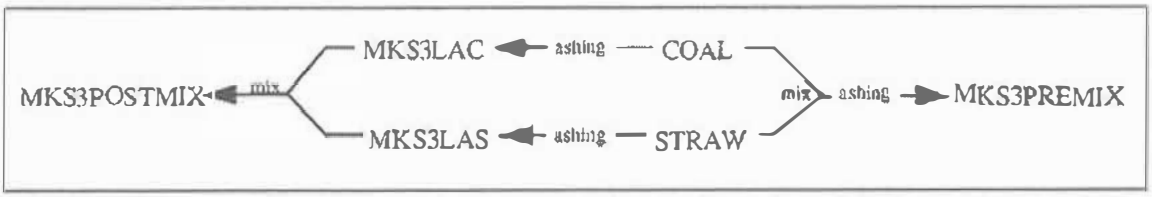

Fig 4.10. Schematic illustration of the laboratory ashes produced from MKS1 experiment 3 fuels: Columbian high volatile bituminous coal and Danish wheat.

MKS3POSTMIX was produced by first ashing the two fuels and thereafter mixing them according to the appropiate energy proportions, based on heating value and ash content. MKS3PREMIX was produced by first mixing the fuels and subsequently ashing the mixture. All ashes were produced at 550°C to avoid large scale loss of volatile elements. All the ashes produced were particulate and was therefore suitable for CCSEM analysis. Selected results for the two mixed laboratory ashes are presented in Fig.4.11 and the full CCSEM results can be found in Frandsen et al. (1998b).

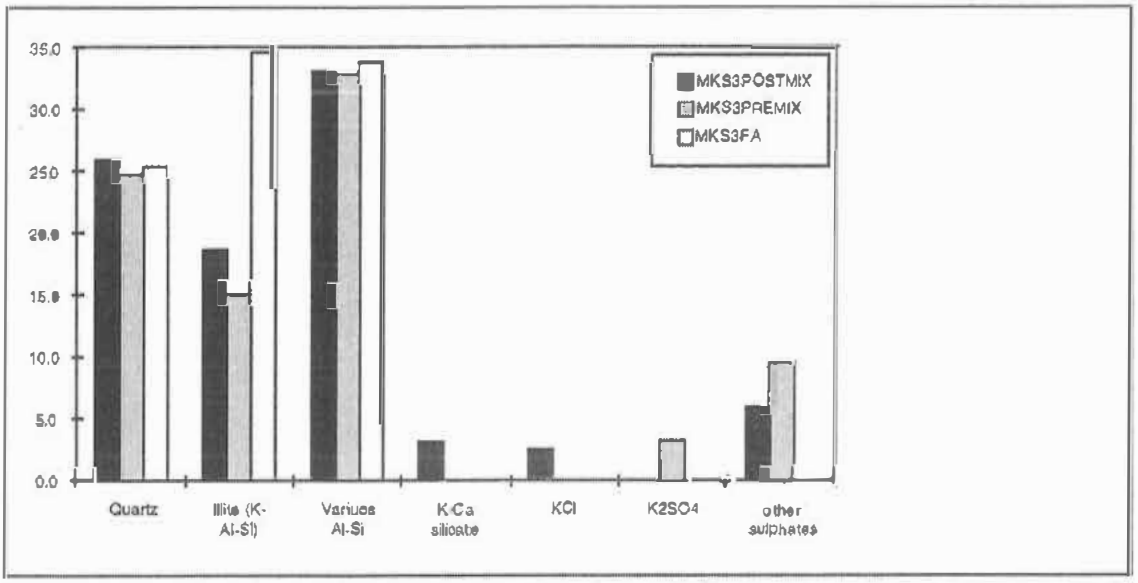

Fig.4.11. CCSEM data for mixed laboratory ashes from MKS1 experiment 3 on a category weight percent basis. For comparison is shown data for fly ash from the same experiment.

From Fig.4.11 it is seen that the two mixed laboratory ashes are quite alike when considering their contents of quartz and various alumino-silicates. However, it appears that while K-Ca silicate and KCl are present in the POSTMIX (separately ashed) these phases are not present in the PREMIX (ashed fuel mixture), which on the other hand contains K_2SO_4 and a higher content of other sulphates. In other words it appears that

the K from the straw preferentially binds to sulphur from the coal when this is present, i.e. in the PREMIX. Additionally, it appears that K-Ca silicates do only form when there are no significant alumino-silicates available for reaction (POSTMIX). This effect is substantiated by CCSEM analyses of fly ashes from co-firing experiments at MKS1 (MKS3FA and MKS4FA) in which no significant K-Ca silicates were observed (Appendix G in Frandsen et al., 1998a).

When examining bulk compositions based on CCSEM analyses, it is seen that the two mixed ashes are quite alike except for the fact that more SO_3 is present in the PREMIX whereas more Cl is present in the POSTMIX (Fig.4.12).

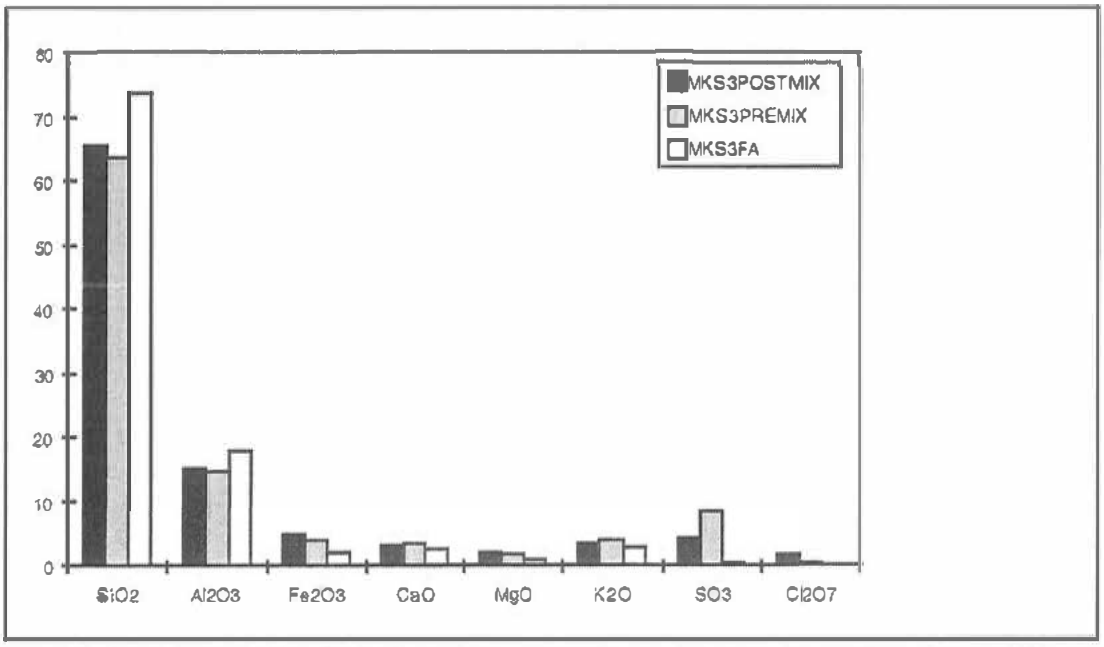

Fig.4.12. Bulk composition (weight percent) calculated on the basis of CCSEM data for the mixed laboratory ashes.

The results of the ashing experiments indicate that whether the laboratory ash is formed by mixing the fuels before ashing or ashing them separately has only slight, but important, consequences for the resulting ash composition since reaction between straw-derived K and coal-derived S to form K_2SO_4 occurs during the ashing. However, compared to fly ash from experiment 3, both ashing procedures yield compositions that are lower in SiO_2 and Al_2O_3 and higher in Cl_2O_7 and SO_3 than the fly ash (Fig.4.12). The K_2O content, however, is similar in the fly ash and in the laboratory ashes.

5. Summary and conclusions

The SEM-study of samples from straw combustion and co-combustion of straw and coal have yielded a reference selection of representative images that will be useful for future comparison. The sample material encompassed potential fuels (wheat straw and grain), bottom ash, fly ash and deposits from straw combustion as well as fuels (coal and wheat straw), chars, bottom ash, fly ash and deposits from straw+coal co-combustion. Additionally, a variety of laboratory ashes were studied.

SEM and CCSEM analysis of the samples have given a broad view of the inorganic components of straw and of the distribution of elements between individual ash particles and deposits. The CCSEM technique does, however, not detect dispersed inorganic elements in biomass, so to get a more complete visualization of the distribution of inorganic elements additional analyses must be performed, for example progressive leaching. In contrast, the CCSEM technique is efficient in characterizing the distribution of elements in ash particles and between ash fractions and deposits.

The data for bottom ashes and fly ashes have indicated that binding of potassium to silicates occurs to a significant extent. The silicates can either be in the form of alumino-silicates or quartz (in co-combustion) or be present as straw-derived amorphous silica (in straw combustion). This process is important for two reasons. One is that potassium lowers the melting point of silica in the fly ash, potentially leading to troublesome deposits by particle impaction and sticking to heat transfer surfaces. The other is that the reaction between potassium and silica in the bottom ash binds part of the potassium meaning that it is not available for reaction with chlorine or sulphur to form KCl or K_2SO_4. Both phases are potentially troublesome because they can condense on surfaces to form a sticky layer onto which fly ash particles can adhere and by inducing corrosion beneath the deposit. It appears that in the studied full-scale experiment of co-combustion of coal and straw, the straw-derived silica were preferentially incorporated in the fly ash relative to the bottom ash.

The analyzed deposits from straw-fired CHP's have shown that in the furnace condensation of KCl is important for formation of the initial layer, whereas building of the outer loose part of the deposit is dominated by particle impaction. Additionally, particle impaction is a more prominent process in the furnace compared to what is the case in the superheater region.

Potassium was observed to react with sulphur preferentially to chlorine and silicate-compounds during low-temperature (550°C) laboratory ashing of a mixture of wheat straw and bituminous coal from MKS3. A similar effect was, however, not observed in full scale fly ashes from MKS3 in which potassium to a high extent have reacted with alumino-silicates to form K-Al silicates. However, potassium sulphates are present in deposits formed during co-combustion at MKS1, especially in the convective pass.

6. Acknowledgements

Fundings from the Danish Energy Research Programme, Elsam and Elkraft are gratefully acknowledged.

7. References

Andersen, K.H., Frandsen, F.J., Hansen, P.F.B and Dam-Johansen, K. (1997). Full scale deposition trials at 150MWe PF-boiler co-firing coal and straw: summary of results. Proc. Eng. Found. Conf.: Impact of Mineral Impurities in Solid Fuel Combustion, Kona, Hawaii, November 2-7, 1997.

Bryers, R.W. (1994). "Analysis of a suite of biomass samples. Foster Wheeler Development Corporation. FWC/FWDC/TR-94/03.

Deer, W.A., Howie, R.A. and Zussman, J. (1966)."An introduction to the rock-forming minerals." Longman Group Ltd.

Frandsen, F.J., Hansen, L.A., Sørensen, H.S. and Hjuler, K., 1998a. Characterization of Ashes From Biofuels. Final Report, Danish Energy Research Programme. Eds. K. Hjuler and H. Sørensen (1998). ISBN 87-7782-000-2.

Frandsen, F.J., Hansen, L.A., Sørensen, H.S. and Hjuler, K., 1998b. EFP-95 project: Characterization of Biomasss Ashes - Data Compilation. CHEC Report No. 9804.

Hansen, L.A., 1997. Ash Fusion Quantification by Means of Thermal Analysis. Presented at the Engineering Foundation Conference on Impact of Mineral Impurities in Solid Fuel Combustion, Kona, Hawaii, November 2-7., 1997.

Hansen, L.A., Frandsen, F.J., Dam-Johansen, K., Sørensen, H.S., Rosenberg, P. and Hjuler, K. (1997). "Ash Fusion and Deposit Formation at Straw Fired Boilers." Proc. Eng. Found. Conf.: Impact of Mineral Impurities in Solid Fuel Combustion, Kona, Hawaii, November 2-7, 1997.

Hjuler, K., 1997. Ash Fusibility Detection using Image Analysis. Proc. Eng. Found. Conf.: Impact of Mineral Impurities in Solid Fuel Combustion, Kona, Hawaii, November 2-7, 1997.

Laursen, K. (1997a). "Advanced Scanning Electron Microscope Analysis at GEUS." Geological Survey of Denmark and Greenland Report 1997/1.

Laursen, K. (1997b). "Characterization of Minerals in Coal and Interpretations of Ash Formation and Deposition in Pulverized Coal Fired Boilers." Ph.D. Thesis, Geological Survey of Denmark and Greenland Report 1997/65.

Marchner, H. (1995) Mineral Nutrition of Higher Plants. 2 Ed., Academic Press (1995).

Morey, G.W., Kracek, F.C. and Bowen, N.L.(1931). "The ternary system K_2O-CaO-SiO_2." Journal of the Society of Glass Technology, Vol.14, pp.149-187.

Olanders, B. and Steenari, B-M. (1995). "Characterization of ashes from wood and straw." Biomass and Bioenergy, Vol.8, No.2, pp. 105-115.

Steenari, B-M. and Langer, V. (1988). "Fasanalys av sintrade och osintrade halmaskor med och utan tillsats av kaolin respektive dolomit." Report OOK 88:12.

Stenholm, M., Jensen, P.A. and Hald, P., (1996). "Biomasses brændsels- og fyringskarakteristika. Fyringsforsøg. EFP-93." 1323/93-0015. (in Danish)

Sørensen, H.S. Computer Controlled Scanning Electron Microscopy (CCSEM) analysis of straw ash. Proc. Eng. Found. Conf.: Impact of Mineral Impurities in Solid Fuel Combustion, Kona, Hawaii, November 2-7, 1997.